Institut Supérieur des Techniques Avancées
Université Jean Monnet
Saint-Etienne

Rapport de fin d'études

Promotion : 2008

Niveau de Diffusion : 03

Filière : INV

Stage du 10/03/08 au 10/08/08

Tuteur : Anne-Claire Legrand

Image processing strategies to extract landmark curves from CT projection data

Mathieu BOUTE

Bone Imaging Laboratory
University of Calgary
2500 University Drive N.W
Calgary, Alberta, Canada
T2N 1N4

Tuteur entreprise : Dr Steven BOYD

1. Acknowledgments

I first would like to express my gratefulness to Dr Steven BOYD for giving me the opportunity of working at the Bone Imaging Laboratory on such an interesting subject. His amazing personality and his great people management skills made the laboratory a nice place to work. I also thank Steven BOYD for supervising my project in its general aspects and spending some time to discuss related issues to it.

I would like to thank Yves PAUCHARD for supervising my project in all its aspects, devoting some of his time to discuss strategies to solve the problem, to help me to overcome some technical difficulties in his usual good mood.

Thanks to Fabio AYRES for always making himself available to other people, and in my case for sharing some views on digital imaging processing.

I would like to thank Shannon BOUCOUSSIS for running the laboratory and helping me in my first days at work, introducing me to other people of the laboratory. I would like to thank Shannon for the time she took for telling me how to deal with the VMS station.

I would also like to thank Graeme, Erika, Kyle, Irene, Dan, Olivia, Samantha, Heather and Helen for sharing, with the people mentioned previously, some good moments off and at work.

I wish you all best of luck in your future projects and hope that the flames will stay longer in the playoffs next year so that we can enjoy some more good times.

2. Summary

Cover page 1

1.Acknowledgments 2

2.Summary 3

3.List of figures 5

4.Introduction 7

4.1. Lab Work 7
a) Presentation of the Laboratory 7
b) Areas of Research 7
c) Scanners used in the Laboratory 9
4.2. General introduction to the subject 10
a) Introduction 10
b) Different types of motion types recorded 10
c) State of the art 11
d) Our method 11
4.3. Scope of Work 12
a) Abstract 12
b) Proposed tasks 12
c) Constraints 13

5.Background in Computed Tomography 14

5.1. Introduction to Computed tomography : 14
a) Data acquisition 15
b) Data processing 15
c) Image Display 16
5.2. Artifacts in Computed tomography 16
a) Sources 16
b) Types and Causes 16
c) Patient Motion Artifacts 17
d) Metal artifacts 17
5.3. Introduction to the Radon Transform 17
a) Definition 17
b) Fourier slice-theorem 18
c) Filtered back-projection 19

6.Methods 20

6.1. Overview of the project 20
d) Starting point 20
e) Use of the "ideal" sinewave 22
f) Extraction of the landmarks in the reconstructed image 22
g) Creation of the ideal sinewave 25
h) Extraction of the actual position of the landmark curve 25
i) default extraction in the high density zone 26
j) link between the two algorithms 26
6.2. The methods 26
a) Conversion of the Data 26
b) Working on the images 26

c) Median Filtering 27
d) Thresholding 1/2 27
e) Thresholding 2/2 28
f) Closing 28
g) Labelization 28
h) Termination of the « big » objects 28
i) Visual inspection 28
j) Centroids 29
k) "Ideal" sinewave 29
l) Threshold 30
m) Search window 30
n) Local maximums 30
o) Matching function 30
p) Default criteria 31
6.3. The experiment 31
a) Model simulated on Matlab 31
b) Validating the model 31
c) Noise model 32
d) ImageJ 33
e) Choice for the different parameters 34
f) Degree of confidence 34

7.Results 35

7.1. Extraction of the landmarks position 35
a) Accuracy of the result 35
b) Comment on the algorithm 37
c) "Funny" fact 38
d) Comment on the parameters used 38
e) Results for this step 39
7.2. Extraction of the landmark curves 41
a) Size of the search window 43
b) Tolerance of the matching function 44
c) Results for this step 44

Conclusion 46

8.Bibliography 47

Mots clefs 48
Résumé 48
Keywords 48
Summary 48

3. List of figures

Figure 1: Location of the bone imaging laboratory.

Figure 2: Health bone architecture (left), osteoporotic bone (right).

Figure 3: Loss in bone density over 12 weeks for ovariectomized rats when compared to controls rats.

Figure 4: Three-point bending test of rat femurs.

Figure 5: Fine Element modeling of bone.

Figure 6: Characteristics of the different scanners used in the laboratory.

Figure 7: Sinogram (raw data from the scanner, left), reconstructed image of the wrist (model created using Matlab, right).

Figure 8 : Sinogram with random motion and reconstructed image.

Figure 9 : Sinogram with continuous motion and reconstructed image.

Figure 10 : Sinogram with Scaling motion and reconstructed image.

Figure 11 : Previsionnal project plan.

Figure 12 : Image rendering in Radigraphy (left) versus Computed Tomography (right).

Figure 13 : External appearance of a CT scan.

Figure 14 :Principle of Computed tomgraphy

Figure 15: CT scanner at the bone imaging laboratory. The patient is put at ease and holders are used to prevent from patient motion during scanning.

Figure 16 : Radon Transform

Figure 17: Sinogram with landmark curves, extracted landmark curves in the sinogram.

Figure 18: Differences between the model (left) and the actual wrist (right).

Figure 19 : Sinogram with six landmark curves.

Figure 20 : Line profile of a projection at a certain angle, the landmark curve position is a local maximum (red dot) that can be easily extracted.

Figure 21: Line profile for a projection at a different angle, the landmark curve is still a local maximum (red dot), but exctracting it from the background will be more complicated.

Figure 22 : Landmark position in the reconstructed image (left), extracted landmarks position (right)

Figure 23 : Extraction of the actual landmark curve position in the sinogram (left) using the « ideal » sinewave (right).

Figure 24: Region of interest in the reconstructed image (in green).

Figure 25 : the three different classes in the image

Figure 26 : only small objects are left (cf right image).

Figure 27 : The extracted landmarks (in blue) perfectly match the different landmark positions.

Figure 28 : Ideal sinewave (in white). Each row (in blue) corresponds to data from projection at angle i.

Figure 29 : The local maximum (red dot) is located in a zone where the extraction process can easily be made (left case), the extraction will be more complex in the second case (bone and landmark overlaping, right case).

Figure 30 : « Phantom image » of the wrist with continuous motion and corresponding sinogram.

Figure 31 : Parameters of the noise for the type of motion: no motion.

Figure 32 : Parameters of the noise for the type of motion: Continuous motion.

Figure 33 : Parameters of the noise for the type of motion: Random motion.

Figure 34 : Parameters of the noise for the type of motion: Scaling motion.

Figure 35 : From the sinogram (left) to the reconstructed image (right).

Figure 36 : From the reconstructed image (left) to the extracted landmarks (right).

Figure 37 : Superimposition of the extracted landmarks and the reconstructed image.

Figure 38 : Selection of the region of interest in the reconstructed image.

Figure 39 : Consequence for the sonogram of the new region of interest (left: original image, right: sonogram of the new region of interest obtained by inverse Radon transform).

Figure 40 : Effects of severe motion on landmarks in the modelization of a wrist.

Figure 41 : Generatd sinewave for landmark 1&2.

Figure 42: Generated sinewave on landmark 3 & 4.

Figure 43: Generated sinewave on landmark 5 & 6.

Figure 44: Landmark curve extracted (green), parameters used: search window of 41, tolerance of 70.

Figure 45 : Landmark Curve extracted in green for a second landmark, same parameters.

Figure 46 : Landmark Curve extracted in green for a third landmark, same parameters.

Figure 47 : Extracted landmark curve with different parmeters (size of the search window : 10, tolerance 70).

Figure 48: Extracted landmark curve with different parameters (search window of 41, tolerance of 20).

4. Introduction

4.1. Lab Work

a) Presentation of the Laboratory

The bone imaging laboratory is located inside the human performance laboratory at the University of Calgary. Its principle investigator and fundator is Dr Steven BOYD, associate professor in mechanical engineering at the University of Calgary. The bone Imaging Laboratory at the University of Calgary is particularly interested in developing quantitative and non-invasive methods to understand the causes of musculoskeletal diseases and injuries.

Figure 6: Location of the bone imaging laboratory.

The laboratory gets funds for its researches mainly from the Alberta Heritage Foundation for Medical Research (AHFMR), the Natural Sciences and Engineering Research Council (NSERC), the Canadian Foundation for Innovation (CFI), the Alberta ingenuity FUND (AIF), and the Undergraduate Student Research Program (USRP).

b) Areas of Research

The laboratory focuses on different areas of research, such as osteoporosis, breast cancer, mechanical testing, fine elements analysis, software development.

The laboratory personally owns three micro-CT scanners to conduct its researches; these materials are especially used because of their non-invasive features, high resolution imaging rendering and possible 3D imaging.

- Research on Osteoporosis :

Osteoporosis is a disease where decreases in bone mass density and quality may eventually lead to spontaneous fracture. By using micro-CT imaging, the laboratory is now able to see differences in bone structures between a healthy human adult wrist to an older, osteoporotic wrist.

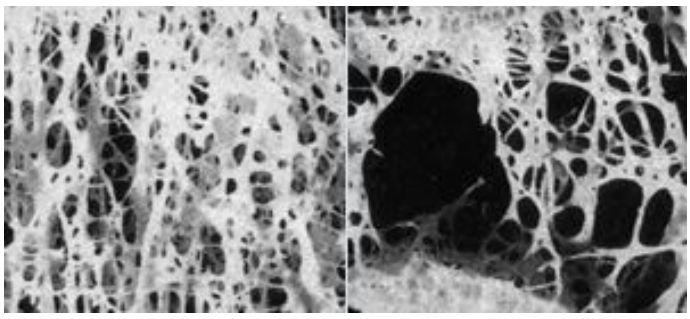

Figure 7: Health bone architecture (left), osteoporotic bone (right).

This technology can be used on the same subject at different intervals of time, the procedure is called a follow-up, it enables us to notice either a decrease in bone mass density, in the case of an osteoporotic patient bone, or a stagnation (or an increase) in the clinical trial of a drug to prevent osteoporosis.

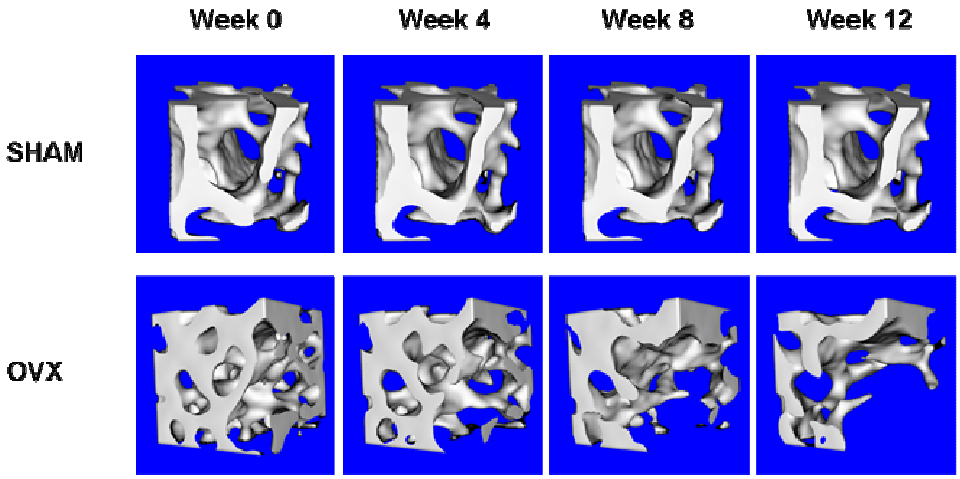

Figure 8: Loss in bone density over 12 weeks for ovariectomized rats when compared to controls rats.

These comparative results are relevant only if the same area of bone is scanned. This is why the images have to be registered prior study. The laboratory is currently working on finding new image registration methods.

- Research on Breast Cancer :

Breast cancer is the most frequent diagnosed cancer in women. One of its consequences is a decrease in the density and structure of the bone that weaken its structure. The laboratory is currently working on image processing techniques to understand the effects of metastasis in the bone structure.

- Research on Mechanical Testing :

Mechanical testing is particularly interesting in bone research as it gives an insight on the bone properties. This can be done by doing three-point bending tests on rat femurs and collect data to establish a fine element model.

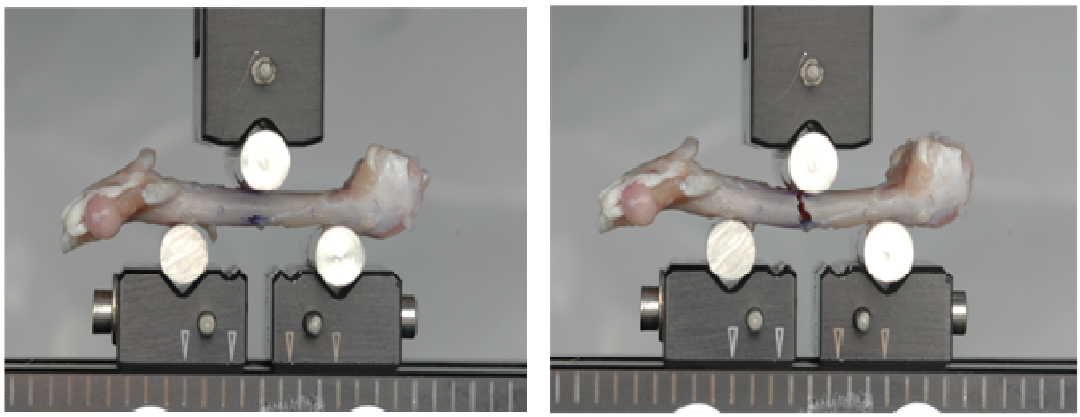

Figure 9: Three-point bending test of rat femurs.

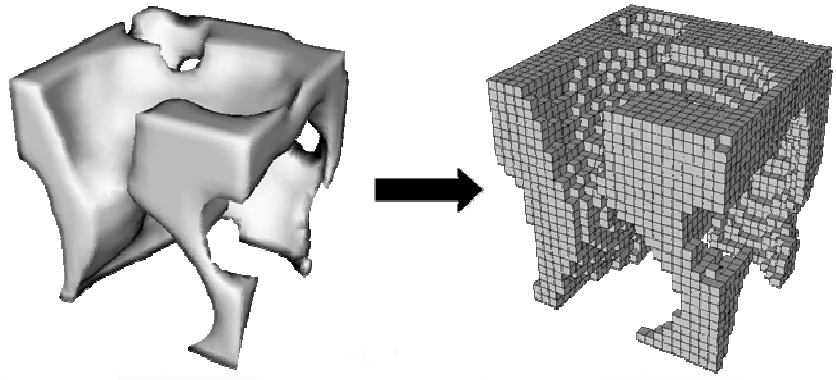

Figure 10: Fine Element modeling of bone.

The laboratory has lately developed an image guided failure device that couples classical mechanical testing as well as micro-CT 3D images of the failure.

- Research on Software Development:

The laboratory regularly develops its own software to extract and interpret informations from micro-CT data. The current "shape software" features registration possibility, 2D and 3D visualizations and fine element modeling.

c) <u>Scanners used in the Laboratory</u>

Scanco Switzerland is the manufacturer of the three micro-CT scanners used in the bone imaging laboratory. The vivaCT40 is used for pre-clinical measurements; the XtremeCT is used for in vivo-patient measurements, where as the micro-CT 40 is used for high-throughput measurement applications. Below are their main characteristics and photographs:

Feature	vivaCT40	XtremeCT	µCT 40
Image			
Type	In vivo (animal)	In vivo (human)	In Vitro
Geometry	Cone-Beam	Cone-Beam	Cone-Beam
Peak/Mean Energy	30-70 kVp/ 20-50 keV	60 kVp/ 40 keV	30-70 kVp/ 20-50 keV
Max. Scan Diameter	20-38 mm	125 mm	36.9 mm
Max. Scan Length	145 mm	150 mm	80 mm
Nominal Resolution	10 µm	42 µm	6- 72 µm

Slice thickness	10-38 µm	41-246 µm	15-90µm
Minimal scan time per slice	3 s	1 s	2 s
Image Matrix	512*512 1024*1024 2048*2048	512*512 up to 3072*3072	512*512 1024*1024 2048*2048

Figure 6: Characteristics of the different scanners used in the laboratory.

4.2. General introduction to the subject

a) Introduction

Artifacts due to patient motion in computed tomography (CT) images are responsible of a loss in quality in the image. This is especially true when using micro-CT to get three-dimensional images of bone architecture. The high resolution capabilities of the scanner and a too long scanning time are responsible for the deterioration of the images.

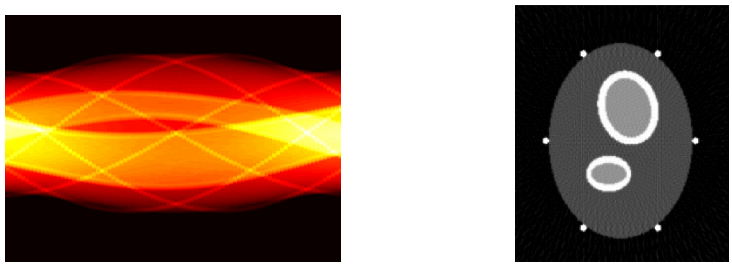

Figure 7: Sinogram (raw data from the scanner, left), reconstructed image of the wrist (model created using Matlab, right).

b) Different types of motion types recorded

Patients are usually asked to cooperate and scanning time can be shortened, when permitted by the acquisition protocol, to diminish artifacts in the images. However, motions still happen and post-processing methods are needed to lessen remaining artifacts.

- Random rigid motion:

The motion is due to the tension of the patient muscles when holding the handle of the arm rest. Below is the 2D slice image of this type of motion.

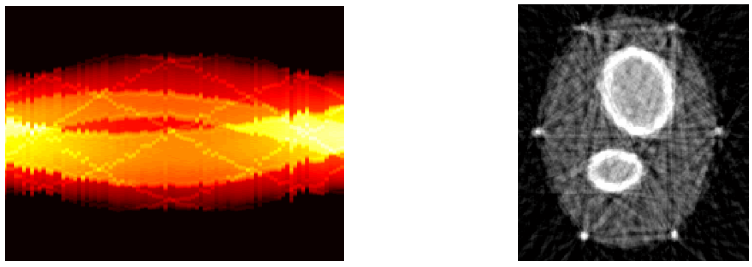

Figure 8 : Sinogram with random motion and reconstructed image.

- Continuous rotation motion:

This type of motion is due to a relaxation of the patient wrist during scanning. The handle is less and less gripped which lead to a continuous motion in the patient wrist. Images of continuous rotation motion can be found below

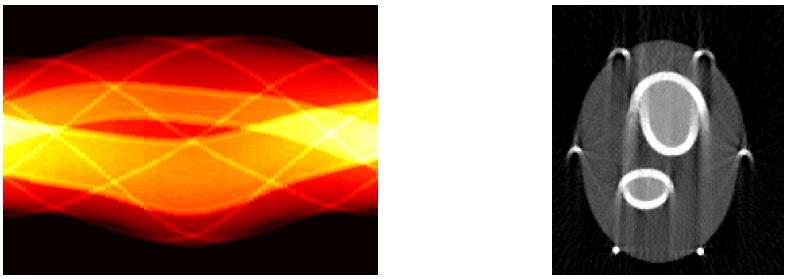

Figure 9 : Sinogram with Continuous motion and reconstructed image.

- Scaling motion:

The scaling motion occurs with living animals. This pseudo-periodic motion corresponds to the animal breathing during scanner. This type of motion will be difficult to diminish because of its origins. However, acquisition can be synchronized with patient breathing to reduce artifacts in images.

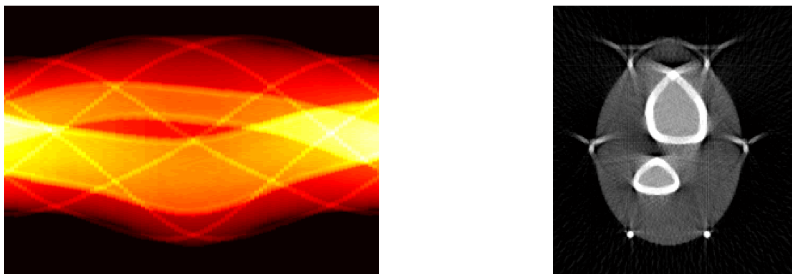

Figure 10 : Sinogram with Scaling motion and reconstructed image.

c) <u>State of the art</u>

A large number of researches have been led to diminish artifacts in images. Most of the actual methods assume a particular motion type. Which is a serious limitation in the case the actual motion doesn't match the model.

The infinite combination of motions (translations, rotations) at different time of the scanning conducts to find a unique motion model for each patient and each acquisition.

d) <u>Our method</u>

Researchers at the bone imaging laboratory are currently working on establishing method for compensating patient motion in computed tomography. The principle of this method is to attach high-density landmarks onto the patient skin and track them into the raw scanner data (sinogram). Without motion present, these extracted landmark curves represent one period of a sine wave in full rotation tomography. If we are able to extract this landmark curves in the sinogram, we will be able to quantify and compensate motion artifacts in µ-CT scan. This extraction step is therefore vital as it is used as a starting point for the compensation.

4.3. Scope of Work

a) Abstract

Patient motion in micro-CT imaging can be quantified and compensated by placing artificial landmarks on the patients skin prior scanning and tracking the position of each landmark in the acquired CT projection data (sinogram). My project consists of implementing different image processing algorithms to extract the landmark position in the sinograms as automatically as possible.

b) Proposed tasks

The subject being clearly defined, my supervisor suggested a certain number of tasks to achieve in order to complete the project. As I was not familiar enough with micro-CT, a familiarization with the topic was necessary. I therefore started by doing a literature review of relevant techniques to compensate for patient motion in micro-CT scan images. This step led to the presentation of a general timeline to achieve the different tasks in time:

- Task 1: Familiarization with the topic.
- Task 2: Presentation of a project plan.
- Task 3: Literature review of relevant techniques.
- Task 4: Implementation of potential techniques in Matlab for 2D tests.
- Task 5: Final implementation possibly using actual scanner projection data.
- Task 6: Final documentation and presentation.

I used the software Gantt project management to present my project plan. Below is a screenshot of the project plan I presented for this project (time-line and tasks).

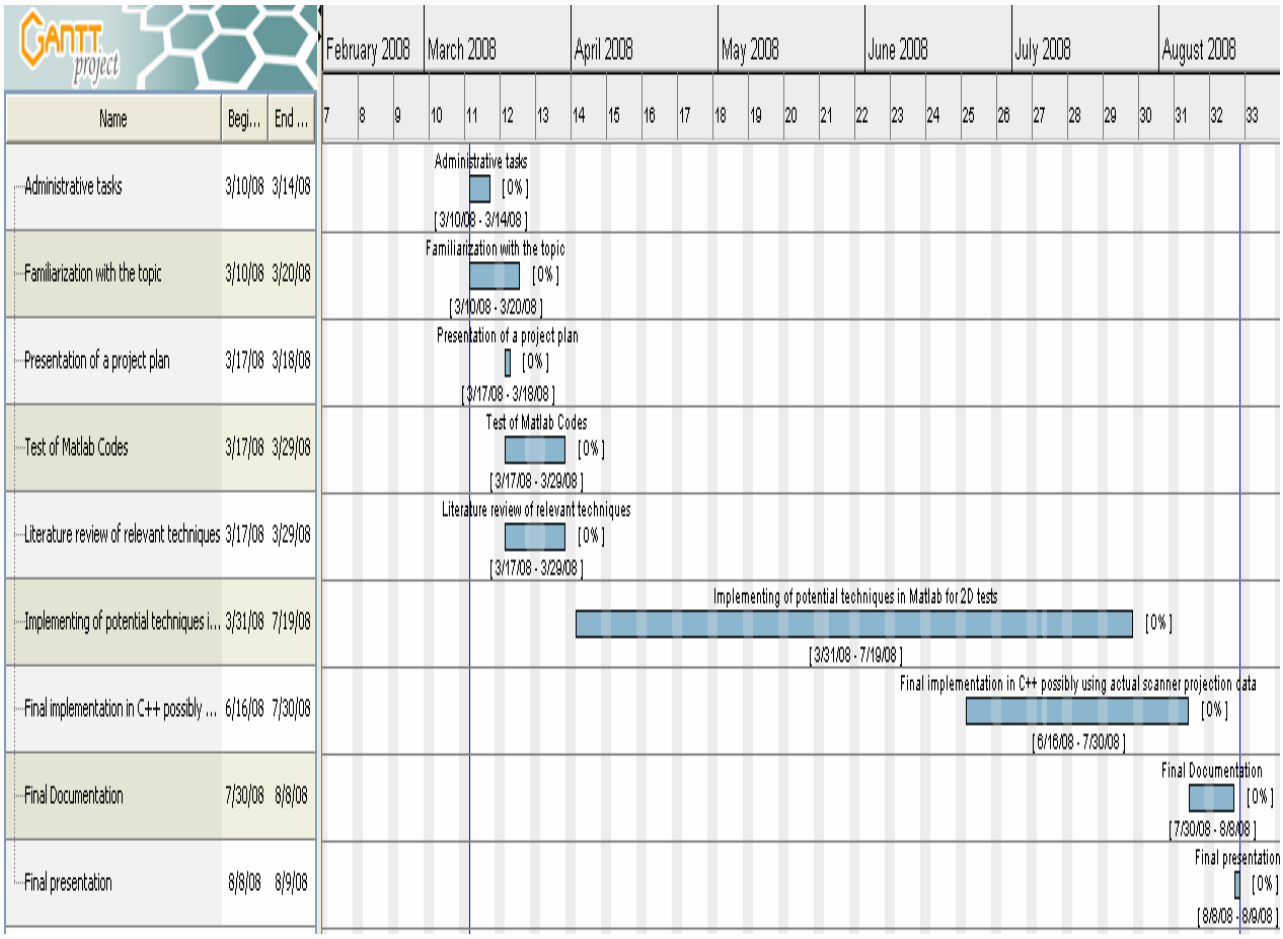

Figure 11 : Previsionnal project plan.

c) Constraints

The aim of this project is to be able to extract landmark curves in micro-CT data. These curves are obtained by putting high-density landmarks onto patient skin before scanning. The landmark curves can more or less be seen easily by human eye, but the operation is subjective, time-consuming and requires a qualified operator for the reading.

The constraints for this project are therefore:

- To extract efficiently the landmark curves as automatically as possible.
- Although no time limit for the processing of the image has been set, it would be relevant that the processing time is as short as possible.
- Data from cone-beam computed tomography scanners will be converted in parallel-bean to be processed.
- The algorithm should start using the image of a sinogram as an input image and the output should be the sinogram with the landmark curves extracted.
- We make the assumption that the landmarks are high density.
- The algorithm should be able to work on 3D sinogram (although it is possible to make it work by taking one slice at a time in a 2D sinogram).

5. Background in Computed Tomography

5.1. Introduction to Computed tomography :

The goal of Computed tomography is to overcome the limitations of radiography and tomography (minimal superimposition, improved contrast, recording of small differences in tissue contrast).

Figure 12 : Image rendering in Radigraphy (left) versus Computed Tomography (right).

The physical principles involve physics and mathematics concepts to understand the way the image is produced, and technologic considerations involve the practical implementation of scientific and engineering principles such as computer science and technology. The physical principles and technology of CT include following processes: data acquisition, data processing, and image display, storage and documentation.

Figure 13 : External appearance of a CT scan.

a) Data acquisition

It refers to the collection of information from the patient to produce the CT image. The two methods of data acquisition are slice-by-slice data acquisition and volume data acquisition.

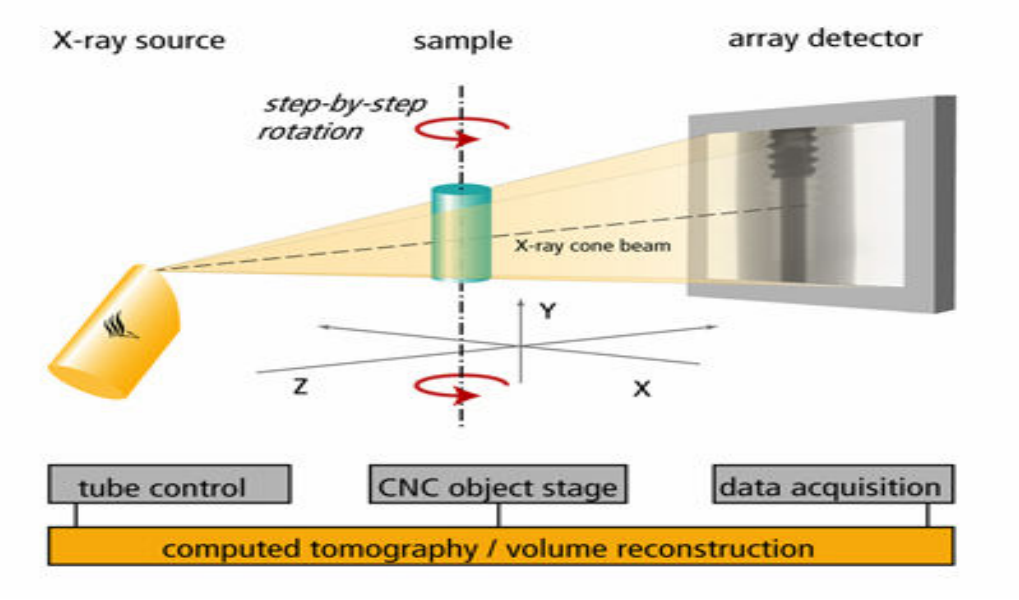

Figure 14 :Principle of Computed tomgraphy

In conventional slice-by-slice data acquisition, data set are collected through different beam geometries to scan the patient. Essentially, the x-ray tube rotates around the patient. The x-ray tube rotates around the patient and collects data from the first slice. The tube stops, and the patient moves into position to scan the next slice. This process continues until all slices have been individually scanned.

In volume acquisition data acquisition, a special beam referred to as helical geometry is used to scan a volume of tissue rather than one slice at a time. In helical CT, the x-ray tube rotates around the patient and traces a helical path to scan an entire volume of tissue. This method generates a single slice per revolution of the x-ray tube.

The first step in data acquisition is scanning. During this time, the x-ray tube and detector rotate around the patient to collect views. The detectors measure the radiation transmitted through the patient from various locations. As a result, relative transmission values or attenuation can be calculated. The relative transmission values are sent to the computer and stored as raw data. The problem in Ct is to determine the attenuation and use this information to reconstruct an image of the slice of tissue. Attenuation is the reduction of the intensity of a beam of radiations as it passes through an object (some photons are absorbed, but others are scattered). The goal of CT scan is to solve the equation: I= $I_0 e$ (in a homogeneous beam), where I is the transmitted intensity, is the original intensity, x the thickness of the object and μ the linear attenuation coefficient.

b) Data processing

Data processing essentially constitutes the mathematical principles involved in CT. Scan data which represent attenuation readings are converted into a digital image characterized by CT numbers.

Conversion of the attenuation readings into a CT image is accomplished by mathematical procedures referred to as reconstruction techniques. Reconstruction techniques include simple back-projection, iterative methods, and analytic methods.

The final step in data processing is image storage of the reconstructed digital image. This image is held in a disk memory as short-term storage.

CT number= $\frac{\mu_x - \mu_w}{\mu_w} K$, where μ_x is the attenuation coefficient of the measured tissue, μ_w is the attenuation coefficient of water, and K is a contrast factor.

c) Image Display

The final step in CT process involves image display, storage, and documentation. After the Ct image has been reconstructed, it exits the computer in digital form. This must be converted to a form that is suitable for viewing and meaningful to the user.

5.2. Artifacts in Computed tomography

Artifacts can degrade image quality and affect the perceptibility of detail. This can cause serious problems for the radiologist who has to provide a diagnosis from the images acquired.

a) Sources

In CT, artifacts arise from a number of sources including the patient, the imaging process itself, and problems relating to the equipment such as malfunctions or imperfections.

Patients who are uncooperative and move during the examination will cause image artifacts. Equipment problems can arise from the system electronics and mechanics and computer algorithms. Additionally, carelessness of the part of the technologist, such as improper positioning of patients in the field of view, will result in image artifacts.

Figure 15: CT scanner at the bone imaging laboratory. The patient is put at ease and holders are used to prevent from patient motion during scanning.

b) Types and Causes

Artifacts in CT can be classified according to cause and appearance. In the classification of artifacts based on their appearance, we can identify four major categories, including streaks, shading, rings, bands, and miscellaneous factors such as the basket weave and Moiré patterns.

Streak artifacts may appear as intense straight lines across an image and may be caused by improper sampler of the data (aliasing), partial volume averaging, motion, metal, beam hardening, etc.

Shading artifacts often appear near objects of high densities and can be caused by bean hardening, scatter radiation, incomplete projections, off-focal radiation, etc.

Rings and bands are caused by bad detector channel in third generation CT scanners.

c) Patient Motion Artifacts

Patient motion can be voluntary or involuntary. Voluntary motion is directly controlled by the patient, such as swallowing or respiratory motion. Involuntary motion is not under direct control of the patient, such as cardiac motion. Both motions appear as streaks that are usually tangential to high-contrast edges of the moving part.

The appearance of streaks results from the inability of the reconstruction algorithm to deal with data inconsistencies in voxel attenuation arising from the edge of the moving part. The computer has difficulty in tracking the location of the voxels.

There are several methods to reduce CT artifacts from motion. It is important to immobilize patients and use positioning aids to make them comfortable and to ensure that patient will stay still during scanning time. Another useful motion artifact reduction technique is to use short scan times for the examination. Concerning motions such as breathing, the technician can also synchronize the scan on patient breathing periods. This type of artifacts will be the focus of the project.

d) Metal artifacts

The presence of metal in the patient also causes artifacts. Metallic materials such as prosthetic devices, dental fillings, and surgical clips give rise to streak artifacts on the image. Metal artifacts can be reduced by the removal of all external metal objects from the patient. Software can also be used to complete the incomplete profile through interpolation. This type of artifacts was mentioned for general knowledge but will not be the focus of the project.

5.3. Introduction to the Radon Transform

a) Definition

In mathematics, the Radon transform in two dimensions, is the integral transform consisting of the integral of a function over straight lines. The inverse of the Radon transform is used to reconstruct images from medical computed tomography scans.

Consider the straight line defined parametrically by :

$(x(t), y(t)) = t(\sin\alpha, -\cos\alpha) + s(\cos\alpha, \sin\alpha)$

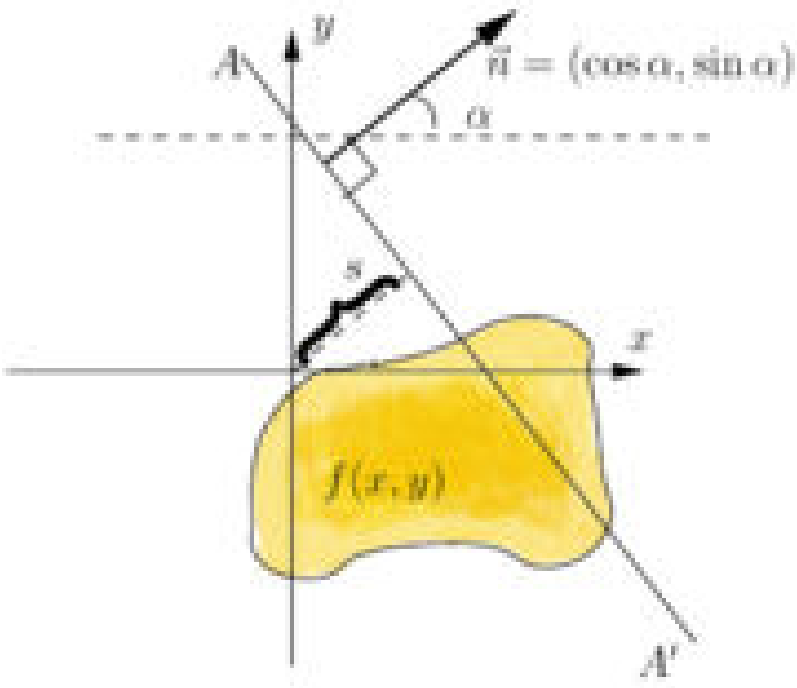

Figure 16 : Radon Transform

Where *s* is the distance from the origin and α is the angle from the *x* axis. We define the Radon transform of a function *f* on the plane (where it is assumed that the function is continuous and vanished outside a disc of some finite radius) by

$$\mathcal{R}[f](\alpha, s) = \int_{-\infty}^{\infty} f(x(t), y(t))\, dt$$

In *n*-dimensional (*n*>2) space the Radon transform is the integral of a function over hyperplanes. The integral of a function over the set of all lines in *n*-dimensional space is called the *X-ray transform* (or ray transform), although it is sometimes loosely referred to as a Radon transform.

In the context of tomography the Radon transform data is often called a sinogram because the Radon transform of a Dirac delta function is a distribution with support on the graph of a sine wave.

Consequently the Radon transform of a number of small objects appears graphically as a number of blurred sine waves with different amplitudes and phases.

This transform in two dimensions and three dimensions (where a function is integrated over planes) was introduced in a 1917 paper by Johann Radon, who provided formula for the inverse transform (reconstruction problem). It was later generalised, in the context of integral geometry.

The Radon transform is useful in computed axial tomography (CAT scan), electron microscopy of small particles like viruses and nuclei, reflection seismology and in the solution of hyperbolic partial differential equations.

b) Fourier slice-theorem

The Radon transform is closely related to the Fourier transform. For a function of one variable we define the Fourier transform :

$$\hat{f}(\omega) = \frac{1}{(2\pi)^{1/2}} \int f(x) e^{-ix\omega}\, dx.$$

and for a function of a 2-vector $\mathbf{x} = (x, y)$

$$\hat{f}(\mathbf{w}) = \frac{1}{2\pi} \int_{-\infty}^{\infty} \int_{-\infty}^{\infty} f(\mathbf{x}) e^{-i\mathbf{x}\cdot\mathbf{w}}\, dx\, dy$$

and for convenience define $R_\alpha[f](s) = R[f](s,\alpha)$ as we will be taking the Fourier transform in the *s* variable. The Fourier slice theorem then states

$$\widehat{R_\alpha[f]}(\sigma) = \sqrt{2\pi}\, \hat{f}(\sigma \mathbf{n}(\alpha)).$$

Where,

$$\mathbf{n}(\alpha) = (\cos\alpha, \sin\alpha)$$

This result gives an explicit inversion formula for the Radon transform, and thus shows that it is invertible on suitably chosen spaces of functions. However it is not particularly useful for numerical inversion.

c) Filtered back-projection

An explicit and computationally efficient inversion algorithm exists for the two-dimensional Radon transform called filtered back-projection. First consider the formal adjoint of *R*:

$$R^*[g](\mathbf{x}) = \int_{\alpha=0}^{2\pi} g(\alpha, \mathbf{n}(\alpha)\cdot\mathbf{x})\,d\alpha,$$

This operator is commonly called 'back-projection' as it takes a function defined on each line in the plane and 'smears' or projects it back over the line to produce an image. Of course this adjoint is not an inverse to the Radon transform, for example the Radon transform of a small object is a function that has a thickened sine wave as its support. If this is back-projected it produces a star like image centered on the original object.

We define a ramp-filter on a function *h* of one variable by

$$\widehat{H[h]}(\omega) = |w|\hat{h}(\omega)$$

then using the Fourier slice theorem and change of variables for integration we find that for *f* a function of two variables, and *g* = *R*[*f*]

$$f = \frac{1}{4\pi} R^* H[g]$$

Which means that the original image *f* can be recovered from the 'sinogram' data g by applying a ramp filter (in the s variable) and then back projecting. As the filtering step can be performed efficiently (for example using digital signal processing techniques) and the back projection step is simply an accumulation of values in the pixels of the image, this results in a highly efficient, and hence widely used, algorithm.

This paragraph is extracted from Wikipedia, it has been included in the report as an introduction to the Radon transform is necessary for somebody starting with computed tomography.

6. Methods

6.1. Overview of the project

d) Starting point

The aim of this project is to extract landmark curves in micro-CT data as automatically as possible. After taking some time to analyze the sinogram image, and understand the properties of its components (the sinogram and the landmark curves), I realized that processing this images would be complex.

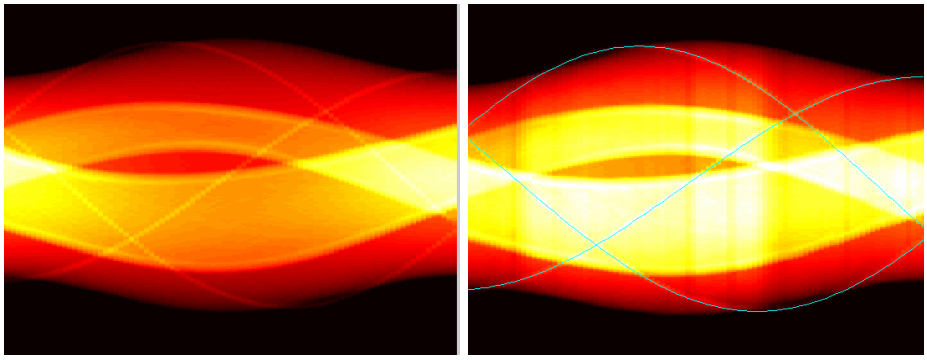

Figure 17: Sinogram with landmark curves, extracted landmark curves in the sinogram.

At this time, I was not working on real micro-CT images, but Yves had been working on creating a Matlab model for the images. The idea was to create a phantom image that would be supposed to look as close as possible from the cross section of a wrist, then performing a radon transform on it to get a modelized sinogram on which I could test my algorithm. The main advantage of doing so is that the size of the image is much smaller than with an actual sinogram image, therefore I could do more tests on it in the same period of time. However, we expected to encounter differences between the model and the actual sinogram image, which would lead to some adjustments in the final algorithm.

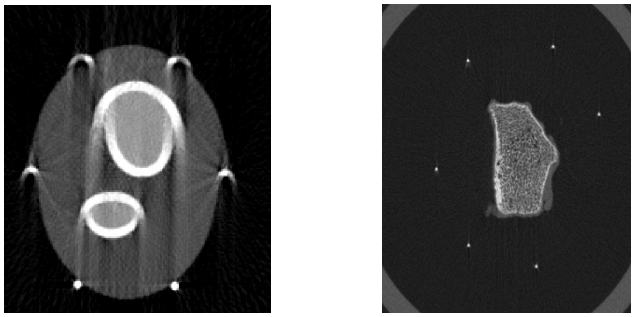

Figure 18 : Differences between the model (left) and the actual wrist (right).

I therefore started to work on this model, and I decided to use the software (ImageJ) to play around with the images to understand and possibly extract some features in the images. It appeared that we could divide the image in two main zones, the first one being the part of the sinogram where the landmark curves does not overlap with the bone architecture (cf figure), and the second one being where the landmark curves overlap with the bone architecture. The landmark curves in the first zone are quite easy to extract as the landmarks are high density and the background surrounding correspond to soft tissues (whose intensity is weaker).

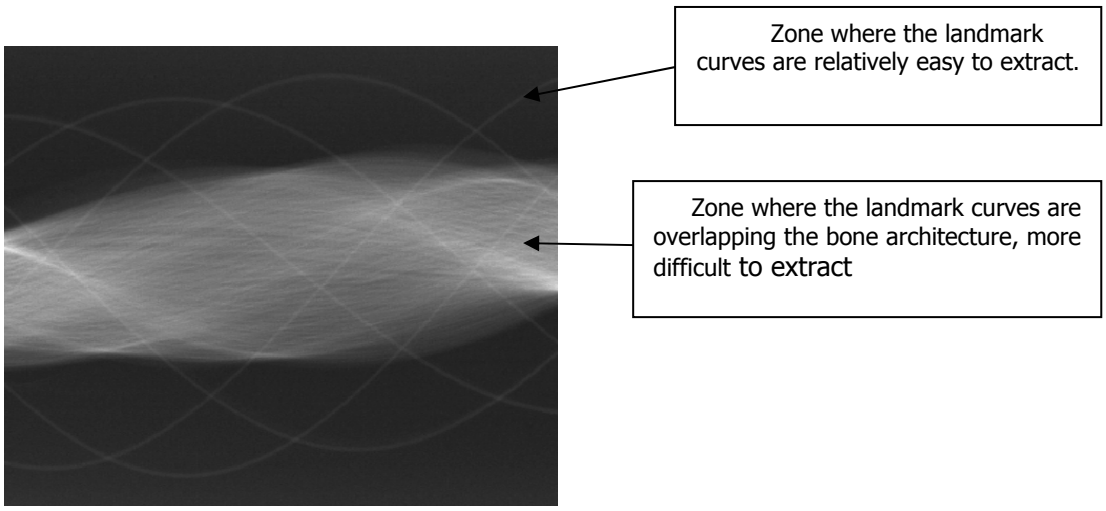

Figure 19 : Sinogram with six landmark curves.

I realized from that point, that I would not be able to process the image directly because of the complexity of the image. In fact, it is very difficult to characterize the landmark curves along the projections. The intensity always changes, and from one zone to another, the intensity gap can be consequent.

However, I noticed two features I could use to extract the landmark curves:

- For any projection, the landmark curve should be a local maximum in its close neighborhood as the landmark are high density.

- If there were no motion, I should get a sinewave pattern for my landmark curve. So even if patient motion occurs during the scan, the landmark curve in the sinogram should follow a sinewave pattern.

These two features have been the starting point of my project, as it was the first time I could characterize these images in some way.

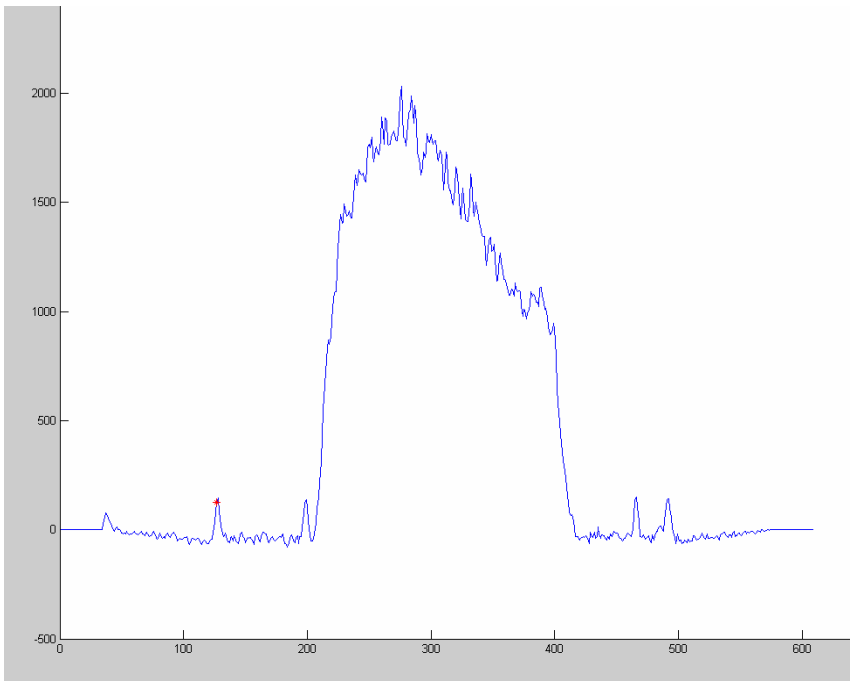

Figure 20 : Line profile of a projection at a certain angle, the landmark curve position is a local maximum (red dot) that can be easily extracted.

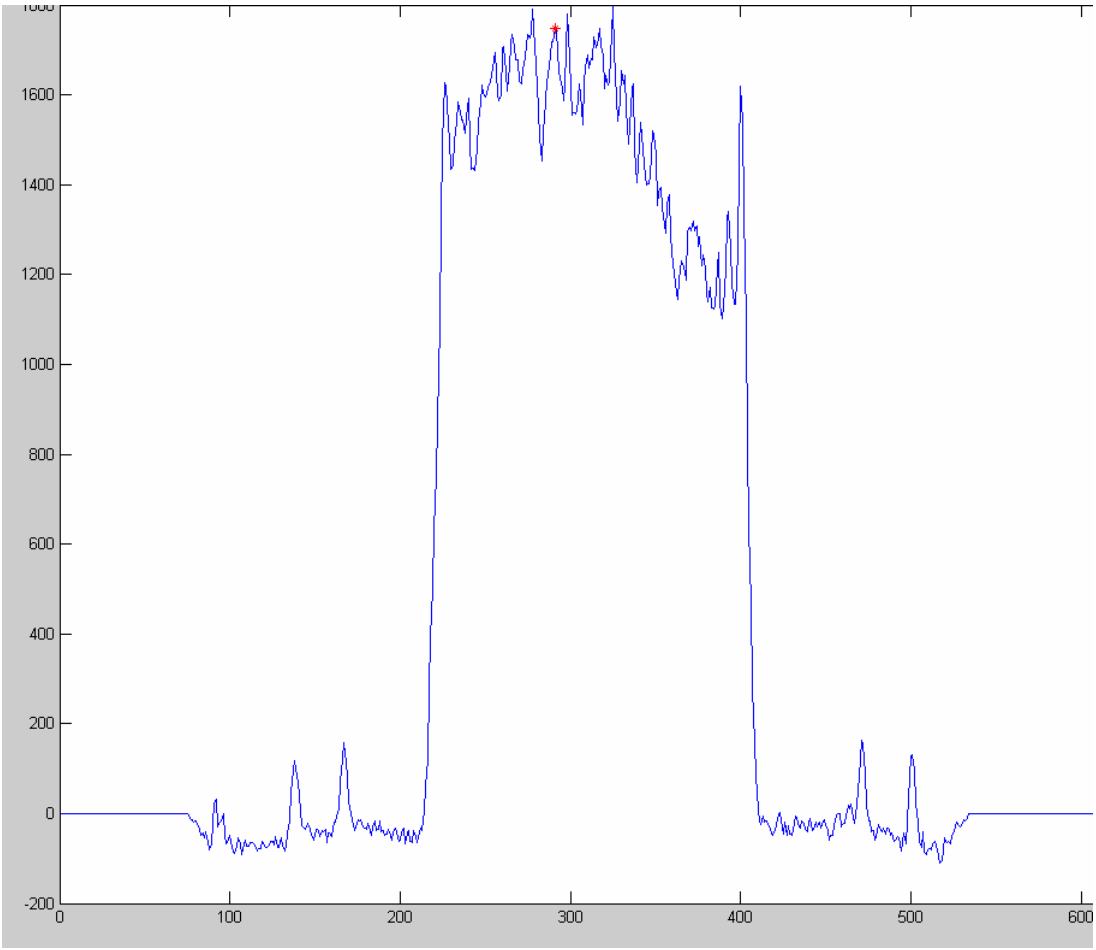

Figure 21 : Line profile for a projection at a different angle, the landmark curve is still a local maximum (red dot), but exctracting it from the background will be more complicated.

e) Use of the "ideal" sinewave

The image being complex, I did not have much information on how to locate and extract the landmark curves in the sinogram. So I used the property of the Radon transform, the fact that it could be inverted.

By extracting the landmark positions in the reconstructed images using a specific algorithm, I performed a radon transform on them to get the "ideal" sinewave. This ideal sinewave corresponds to the sinewave I would get in the sinogram if there were no motion occurring during scan time. This ideal curve is very helpful as it gives me a mean position to find the landmark curves. I expect the landmark curves position at different angles, to be in a close neighborhood of the "ideal" sinewave.

f) Extraction of the landmarks in the reconstructed image

Different steps will be necessary to extract the landmarks in the reconstructed image, all of them will be explained and justified in detail in the following part (5.2 the methods).

My algorithm starts with the use of a median filter to reduce the noise while preserving the details in the image. The image will then be thresholded, using the maximization of the variance interclass which will threshold the images automatically. At this point, I will only have three types of objects: the background, the soft tissues, and the high density components e.g., the bone and the landmarks. Only this class is of an interest to me, therefore I perform another threshold to get rid of the others. The next step consist in performing an closing on the image (dilation + erosion) to get rid of the small components in the image that are not the landmarks (these elements are especially found in the bone

and constitute its structure, it is called the trabecularr). After labelizing the objects remaining in the images, I am able to extract the landmarks positions by terminating the object whose surface is superior to a parameter corresponding to the surface of the landmarks.

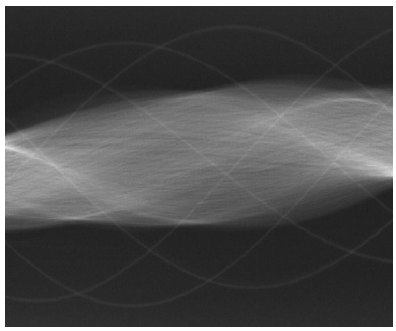

Input image : Sinogram

Inverse Radon

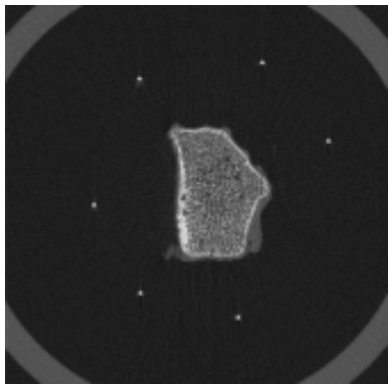

Reconstructed Image + Median Filter

Thresholding (maximization of the interclass variance)

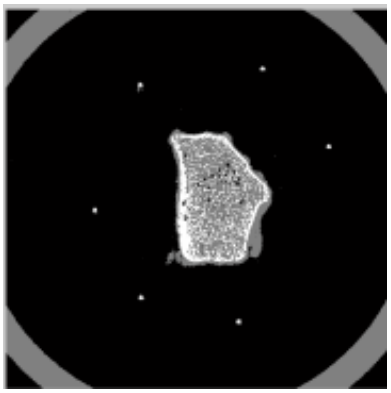

Thresholded Image (3 classes)

Manual Thresholding

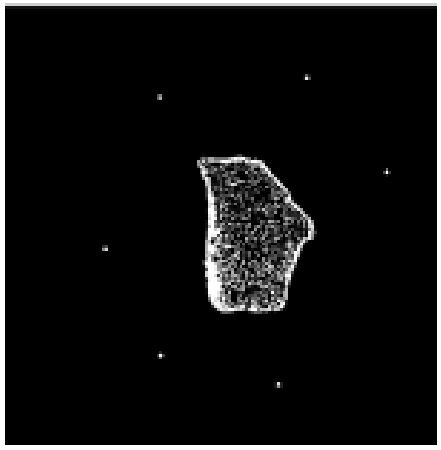

Thresholded Image (2 classes)

Closing (dilation + erosion)

Image after closing operation

Termination of "big" objects

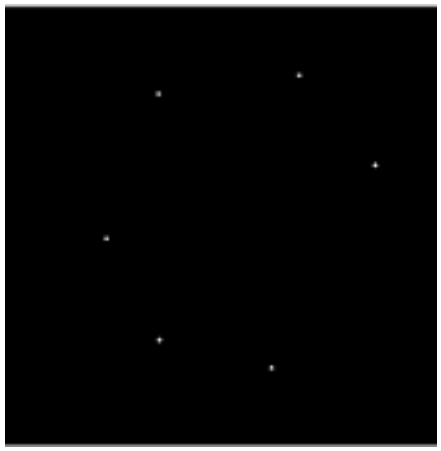

Extracted landmarks

g) Creation of the ideal sinewave

At this point of this algorithm, I already extracted the landmark positions in the reconstructed image.

Figure 22 : Landmark position in the reconstructed image (left), extracted landmarks position (right)

I will now labelize the image to be able to work on the landmark one at a time.

I then perform a Radon transform on each of them, the result of this operation is a perfect sinewave, that I will use in an other algorithm to extract the landmark curves in the sinogram.

h) Extraction of the actual position of the landmark curve

In order to extract the landmark curves in the sinogram, I decided to use the results I had obtained previously. In fact, I know where I expect to find the landmark curves thanks to my previous algorithm to get the "ideal" sinewave. The idea is therefore to move along this sinewave one projection at a time and use a search window which is actually a column vector.

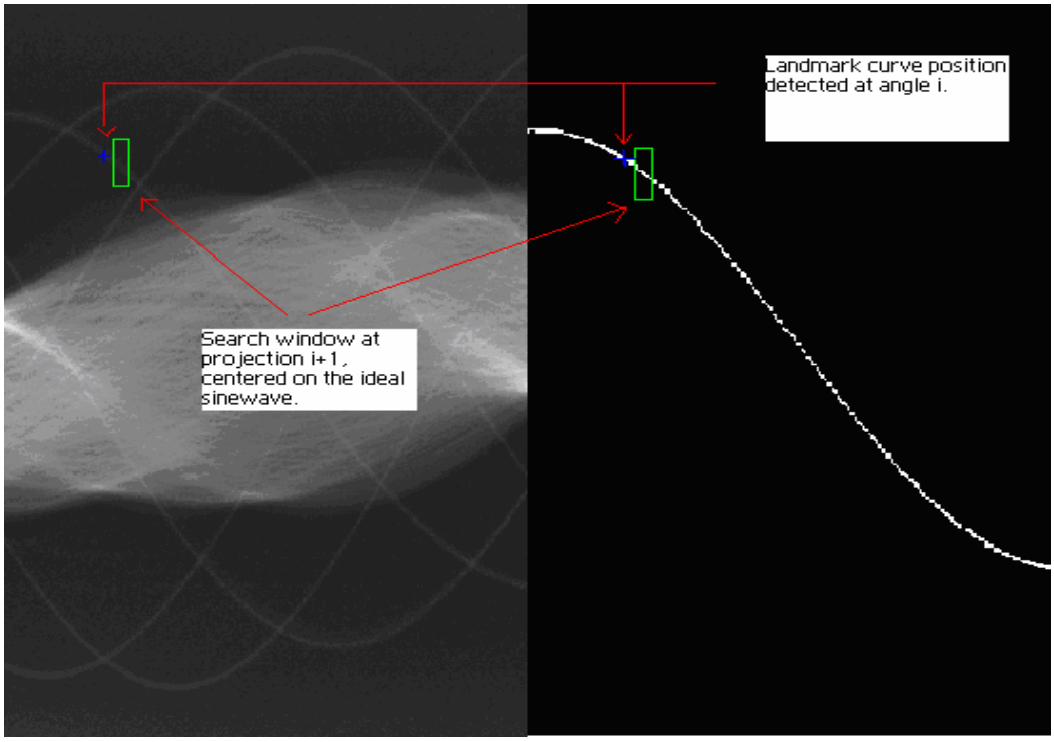

Figure 23 : Extraction of the actual landmark curve position in the sinogram (left) using the « ideal » sinewave (right).

The column vector can be easily modified; its size will be determined by the intensity of the patient motion expected. From this point, I use one of my assumptions which is that, as the landmarks are high density, I expect them to correspond to a local maximum in my column vector. Therefore, the numbers of candidates for the actual position of the landmark curve is restricted to the local maximums in my search window.

I now need to know which local maximum correspond to the actual position of the landmark curve or at least which one is the most likely to correspond to it.

The second assumption I made is now used. I do not expect the landmark curve to change radically from one projection to the next one. Therefore, if I am able to find the position of my landmark curve at projection i, I will be able to determine which local maximum of my window search at projection i+1 is the most similar. Using this matching function, the ideal sinewave and the two assumptions, I will be able to extract the landmark curves position.

i) default extraction in the high density zone

As I mentioned previously, when approaching the high density zone of the sinewave, the extraction becomes more difficult. The fact that I track the landmark position from one projection to the following one can lead to a wrong result, especially in the high density zone. Therefore if my matching function does not work or gives more result than expected, I will give a default result. This default result corresponds to local maximum which is the closest from the center of my search window.

This default result presents the advantage to re-center my window search on the center of the ideal sinewave and acts as a starting point for the rest of the tracking algorithm.

j) link between the two algorithms

One constraint of the project is to make the extraction process as automatic as possible. The first algorithm uses a sinogram image as an input image, reconstruct it to get the cross section of the scan object, and process the image to extract the landmarks positions. The second algorithm enables me to find the position that is the most likely to be the actual position of the landmark curve given the previous position of the actual landmark curve.

The first algorithm can be linked with the second one, by using the position of the extracted landmark, performing a radon transform on it, and apply the default extraction algorithm on the first row of the sinogram, which will be the starting point for the second tracking algorithm.

6.2. The methods

In this part, I will explain in more details, all the functions I used for my different algorithms.

a) Conversion of the Data

The images from the scanner have to be converted to an exploitable file format in Matlab so that, they can be processed.

Images acquired from the scanner at the bone imaging laboratory are at the format RSQ, it corresponds to the raw data from the scanner. Scanco has a software that enables conversion from Cone-Beam sinograms to Parallel-beam sinograms. The file format can therefore be changed from RSQ to PSQ. The sinogram can now be converted into a DICOM file that can be used in Matlab.

b) Working on the images

Medical images usually take a consequent storage size. In the case of the images I have been working on (images of the wrist of a patient), one slice of a 3D sinogram (e.g. a 2D sinogram) is too big to be displayed entirely in Matlab. The first step of the algorithm will be to resize the image to half of its size for the tests. This also has the advantage to make the processing faster.

The original size for a sinogram was 750*1536, it is now 375*768.

The presence of elements in all the four corner of the reconstructed image generates a sinewave pattern (when performing an inverse Radon transform) in the sinogram image that hinders the readings. I consequently decided to only choose a region of interest that would not take them into account.

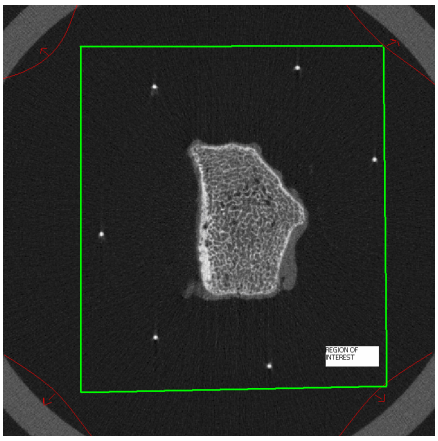

Figure 24: Region of interest in the reconstructed image (in green).

The size of the reconstructed image will be 444*411 and the size of the corresponding sinogram will be 375*609, 375 being the number of projections.

c) Median Filtering

Median filtering is a nonlinear operation often used in image processing to reduce "salt and pepper" noise. I used this type of filter to reduce noise and preserve edges. The structuring element was a 3*3 matrix.

d) Thresholding 1/2

To extract the landmark position in my reconstructed image, I needed to threshold the image. I chose the threshold using the maximization of the interclass variance with three classes as it is an automatic threshold (which is one of my constraints) that takes into accoun the particularity of the images.

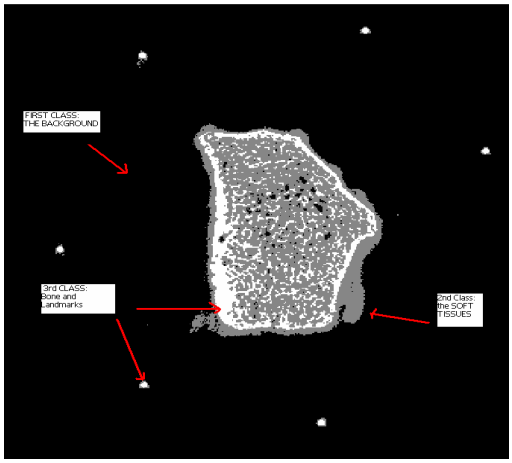

Figure 11 : the three different classes in the image

The number of classes was set to three as there are three main classes in the images: the background, the soft tissues and the high density components (bone and landmarks). Trying to

differenciate the landmarks from the bone would not have been possible as the two of them are really close in intensity.

e) Thresholding 2/2

The previous step set the different classes at different grey levels. The background was set to zero, the soft tissues to 0.5 and the landmarks and the bone to 1. We only have to treshold the result image at any treshold within] 0.5 ; 1[. I personnaly chose 0.7. The only objects in the result image are the landmarks and the bone architecture.

f) Closing

Closing is a dilation followed by an erosion operation. The objective of this operation is to make the small component of the bone architecture (trabercular) grow so much that they merge and become one big object. This big object will be terminated later by a surface parameter. I chose a squared shape structuring element with a size of 30*30. The second step of the closing (the erosion) enables objects that have not merged with others to get back to their original size (if the landmark does not look exactly as before it does not really matters as the only objective of this algorithm is to get the centroid of the different landmarks).

g) Labelization

Now that the landmarks and the bone are clearly separated from the background, I labelize the image, e.g. I give a number to all the objects present in the image. This number will enable me to access one object in particular and perform operatons on it.

h) Termination of the « big » objects

Now that the all the objects have been labelized, I can access them and get rid of the one whose area is bigger than 200 pixels. This number is a bit bigger than the size of my landmarks. Therefore only the objects smaller than 200 pixels will be left in the image, e.g. the landmarks

Figure 26 : only small objects are left (cf right image).

i) Visual inspection

The landmarks extracted can be compared visually with the original reconstructed image, by using them as a mask on it.

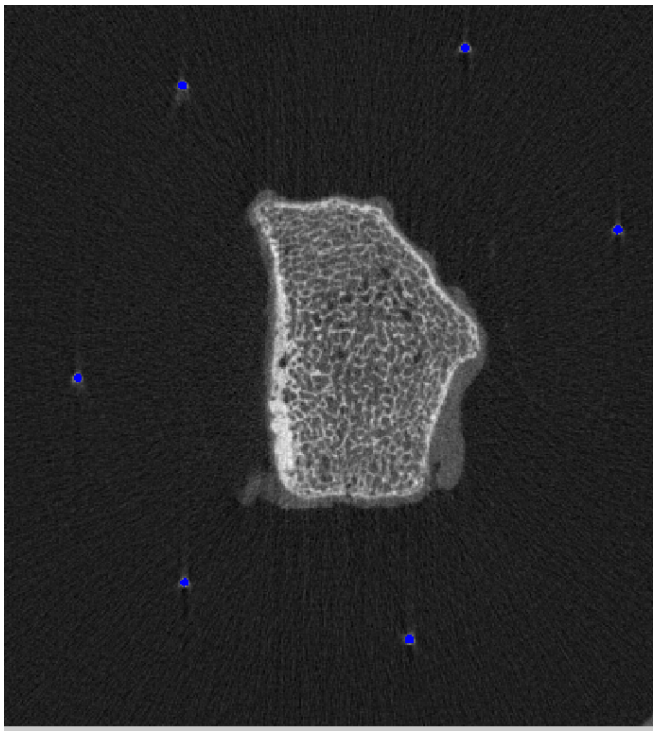

Figure 27 : The extracted landmarks (in blue) perfectly match the different landmark positions.

j) *Centroids*

After labelizing the image once again, I find the centroid of each landmark and save the coordonates for a future use. The coordonates may not always be an integer; I therefore round each coordonnate to the closest integer so that I will be able to access and display them.

k) *"Ideal" sinewave*

Without motion present, these extracted landmark curves represent one period of a sine wave in full rotation tomography. By creating a matrix of zeros of the size of the reconstructed image and by putting only one pixel to one (the one corresponding to the desired landmark position), I can generate the "ideal" sinewave corresponding to this landmark by performing a radon transform on the image. The result of this operation indicates the mean value of the landmark curve in the sinogram.

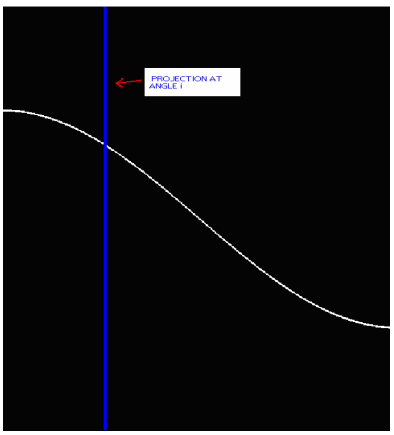

Figure 28 : Ideal sinewave (in white). Each row (in blue) corresponds to data from projection at angle i.

l) *Threshold*

When I performed the Radon transform on the landmark position, it created an image of a sinewave. However this image was not a binary image, so I thresholded the image manually (threshold value = 0.0001) to binarize the image.

m) *Search window*

Considering I have extracted the landmark curve position at angle I (or projection i), I expect the landmark curve position at angle i+1 to follow the trend of my ideal sinewave. If a motion should occur during scanning, the exact landmark curve position for projection i+1 should be in the neighborhood of the ideal sinewave. This is the reason why I created the concept of the search window. The search window is a column vector of size 41*1, centered on the ideal sinewave. The size has been determined after study of the different motion I had in all the images available.

By moving the search window along the sinewave, I am able to record a number of possible locations for the landmark curve, given that the size of the search window was properly set.

n) *Local maximums*

One of the first hypotheses was that the landmarks are high-density. I therefore assume that in all the possible location for the landmark curve at projection i, only the ones corresponding to a local maximum in the search window is a possible location. This criteria diminishes the number of possible applicants from the size of the search window, to the number of local maximums in the column vector.

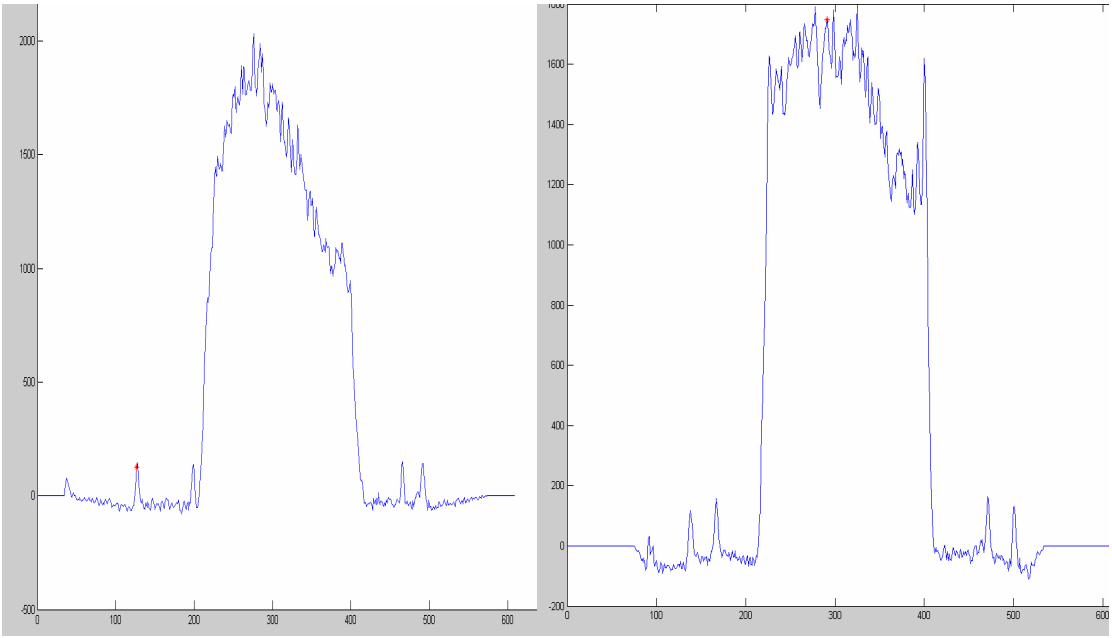

Figure 29 : The local maximum (red dot) is located in a zone where the extraction process can easily be made (left case), the extraction will be more complex in the second case (bone and landmark overlaping, right case).

o) *Matching function*

I made the hypothesis previously that for one landmark curve position in a projection to the next landmark curve position in the next projection, the intensity of the pixels should not change by much. This part of the algorithm can be compared to the tracking algorithm called: optical flow.

So if I know the position of the landmark curve at angle i and its intensity, and I have a selection of possible locations for the landmark curve at angle i+1 (that I obtained thanks to the ideal sinewave and the locam maximum criteria), I am able to use a matching function to determine which position is the most likely to be the position for the landmark curve at this projection.

The matching function requires as input parameters : the pixel coordinates corresponding to the landmark curve at projection i, its intensity, and a tolerance corresponding to the maximum change of intensity between the landmark curve position at angle i, and at angle i+1. The ouput parameter will be the index of the position in the search window, which will make us able to access the coordonnates of the pixel at angle i+1, and its intensity. This will be used as a starting point for the next projection.

In the case that there is a problem with the detection of the landmark curve position, e.g. if two many or none possible candidates are found, the algorithm will use a default criteria to still produce a result.

p) Default criteria

The algorithm to work must only have one parameter in output of the matching function, as the algorithm uses the output as an input for the next projection. If there are more than one parameter or if there are not any, the algorithm will be stop at the current projection.

In the zone where the landmark curve overlaps the bone architecture, this is very likely to happen, as well as when two landmark curves are about to cross each other.

The default criteria is likely to be used in this two cases.

The idea of the default criteria is to find among the different local maximum extracted in the search window, the one who is the closest from its center. This enables the algorithm to keep on working to its end while still giving and ouput result that is a possible location for the landmark curve position.

The defaut criteria also allows to recenter the matching function along the ideal sinewave.

6.3. The experiment

In this part, I will explain what experiments I did to validate the algorithms I used to extract the landmark curves.

a) Model simulated on Matlab

Before I started my internship at the bone imaging laboratory, Yves Pauchard had been working on creating a model of the wrist on Matlab, so that, patient motion could be simulated on it. I therefore used this model for the first part of my project. The objective was to find an extraction algorithm that worked on the model as the time for processing the images would be much shorter that if I were using actual images. Even if differences exist between the model and the actual images, the algorithm found in the first case should not have to be changed by much to be applied to the second case, the actual images.

b) Validating the model

The first step of the project was therefore to make sure that the model corresponds as much as possible to the reality.

In the final algorithm, the objective is to start with a sinogram as an input image. However, constructing a model of a sinogram is more complicated than creating a model of the reconstructed image. The model was therefore obtained by creating the "phantom image" and by performing a radon transform on it to get a sinogram.

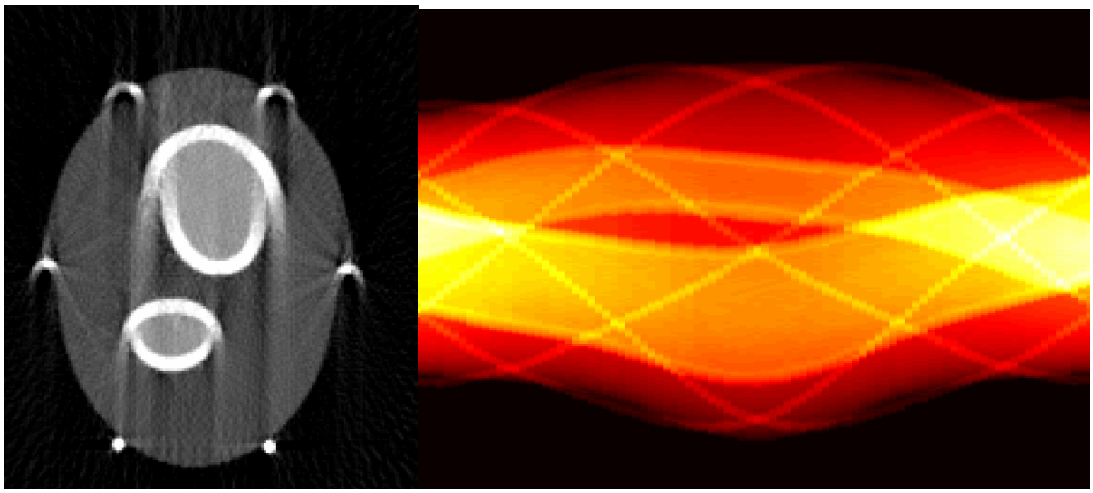

Figure 30 : « Phantom image » of the wrist with continuous motion and corresponding sinogram.

The "phantom" image is quite similar to what we can expect from the cross section of a wrist, as different zones can be recognized. The two big white circles represent the edges of the bone inside the wrist. We can distinguish a grey zone inside these circles that would correspond to the trabercular that can be found into a bone. The darker grey zone corresponds to the soft tissues (the skin and muscles), and the high density landmarks are show mainly in white. The model created is visually similar to the actual wrist of a patient.

c) Noise model

However, the noise model had to be changed. In fact, when we decided to use the phantom image and take its radon transform to create the model of the wrist, the result with the sinogram image was not satisfaying. Different sinewave pattern would appear in the image. This was due to the fact that the Gaussian noise was directly added to the "phantom" image. So when doing the Radon transform, the pixels concerned by the noise would generate a sinewave pattern in the sinogram. The solution to this problem was to create the model of the wrist first, apply the desired type of motion (no motion, continuous motion, random motion, scaling motion), then calculate the projection at different angle (Radon transform) and eventually adding the noise to the sinogram.

The algorithm selected to extract the landmark position from the model images was tested between different values for the variance and the mean of the noise, and for different types of motions:

Noise parameters	**Value of the variance**					
Value of the mean		0.1	0.01	0.005	0.0002	0.0001
1		No	No	No	No	No
0.1		yes	yes	yes	Yes	yes
0.01		Yes	yes	yes	yes	Yes
0.001		Yes	Yes	Yes	yes	Yes
0.0001		yes	Yes	Yes	yes	yes

Figure 12 : Parameters of the noise for the type of motion: no motion.

Noise parameters	Value of the variance					
Value of the mean		0.1	0.01	0.005	0.0002	0.0001
1		No	No	No	No	No
0.1		No	yes	yes	Yes	yes
0.01		No	yes	yes	yes	Yes
0.001		No	Yes	Yes	yes	Yes
0.0001		No	Yes	Yes	yes	yes

Figure 32 : Parameters of the noise for the type of motion: Continuous motion.

Noise parameters	Value of the variance					
Value of the mean		0.1	0.01	0.005	0.0002	0.0001
1		No	No	No	No	No
0.1		No	No	yes	Yes	yes
0.01		No	No	yes	yes	Yes
0.001		No	No	Yes	yes	Yes
0.0001		No	No	Yes	yes	yes

Figure 33 : Parameters of the noise for the type of motion: Random motion.

Noise parameters	Value of the variance					
Value of the mean		0.1	0.01	0.005	0.0002	0.0001
1		No	No	No	No	No
0.1		No	No	yes	Yes	yes
0.01		No	yes	yes	yes	Yes
0.001		No	Yes	Yes	yes	Yes
0.0001		No	Yes	Yes	yes	yes

Figure 34 : Parameters of the noise for the type of motion: Scaling motion.

d) ImageJ

I used the software ImageJ to try different morphological operations on the image. The aim of this step is to get an insight of how the image would react to the processing and elaborate a strategy. ImageJ was chosen as a software for the test for its ability to deal with different formats of images, and the fact that many functions can be uploaded from internet and integrated in the software. The software only works with the images of the model as the actual dicom files from the scanner is too big to be used with it.

Different algorithm were used, like performing a top-hat operation (result of an opening substracted to the result of a closing) on the image to correct for the change of lighting in the image, then doing a laplacian to extract the landmark curves. The result of this operation was interesting in the area where the landmark curve does not overlap the bone architecture, but it was not efficient elsewhere. Other operations were tried, but their result was not relevant as it does not take care of the specificities of the image.

Therefore, I decided to use the reconstructed image, to extract the landmarks position and have an approximation of the mean value for the landmark curve at each projection.

e) Choice for the different parameters

The first step of the algorithm consists in extracting the landmarks position from the reconstructed image. The second one consists in finding the actual landmark position, thanks to a specific algorithm, using the landmark curves obtained from the extracted landmark in the first algorithm. Each operation has been validated and their conditions of use are stated below.

- Median filtering: The filter used was a 3 by 3 matrix. The bigger the size is, the more difficult the extraction of the landmark after the thresholding operation will be.
- Thresholding: 3 classes were used for the thresholding as it corresponds to the number of different types of element you can find in an image. Because of the complexity of the image, a higher number of classes would lead to some false detections.
- Closing: A squared shape structuring element with a size of 30*30 was chosen. The size of the structuring element has to be less than the distance between the landmarks or between a landmark and another object to prevent them from merging.
- Termination of the big object: Objects whose area is under 200 pixels will be kept; the size for this criteria has to be higher than the size of the landmarks.
- Search window size: The size of the search window has to be big enough to contain the actual position of the landmark curve when motion occurs. The size of 41 pixels was chosen to fit most patient motion. This parameter has a big importance on the rest of the algorithm as it restrains the number of possible locations to the size of the search window.
- Tolerance: This parameter is used in the matching function. If the tolerance is too big, the exctration is very likely to be wrong, whereas if it is too small, the defaut criteria will be used, preventing the algorithm from really detecting the actual landmark curve position. A tolerance of 70 offers the best results for the sinogram images.

f) Degree of confidence

The algorithm uses a sinogram image as an input image and extracts the landmark curves from it.

The output image will have extracted landmark curve position from the matching function and from the defaut criteria. In order to know, for each landmark, the number of positions extracted by the defaut criteria and by the matching function, a binary vector is created. If the matching function is used for the extraction process, then a one will be added and a zero else.

This step gives some statistical analysis, and enables us to know, where the detection was more difficult.

7. Results

7.1. Extraction of the landmarks position

The first step of the algorithm is to extract the landmarks position in the reconstructed image. This step was made necessary because of the complexity of the sinogram image.

As the input image, is the sinogram, an inverse radon transform was performed to start with the image of the cross-section of a wrist.

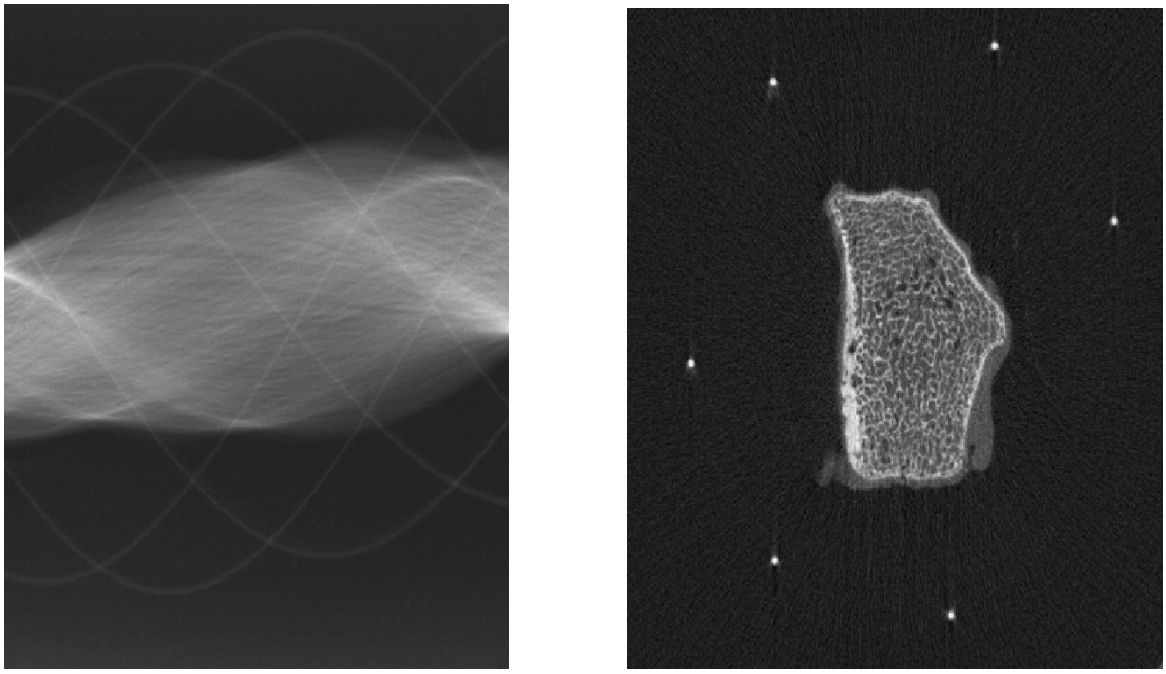

Figure 35 : From the sinogram (left) to the reconstructed image (right).

a) Accuracy of the result

The results were obtained by taking different frames of the dicom file and running the algorithm.

The landmark position was correctly extracted. In fact, the centroids of the exctracted points perfectly match the position of the landmarks in the reconstructed image. This can be seen on the figure below:

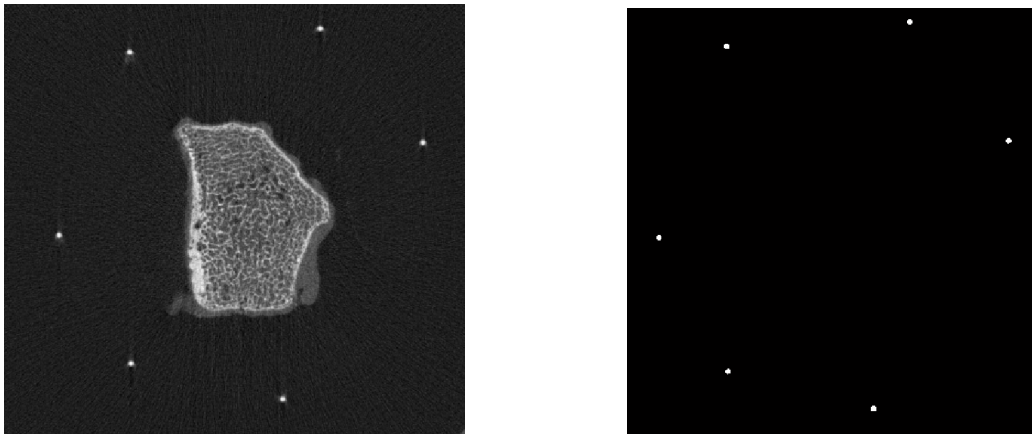

Figure 36 : From the reconstructed image (left) to the extracted landmarks (right).

By putting on the same image the extracted landmarks and the reconstructed image, we can appreciate the quality of the extraction of the landmarks.

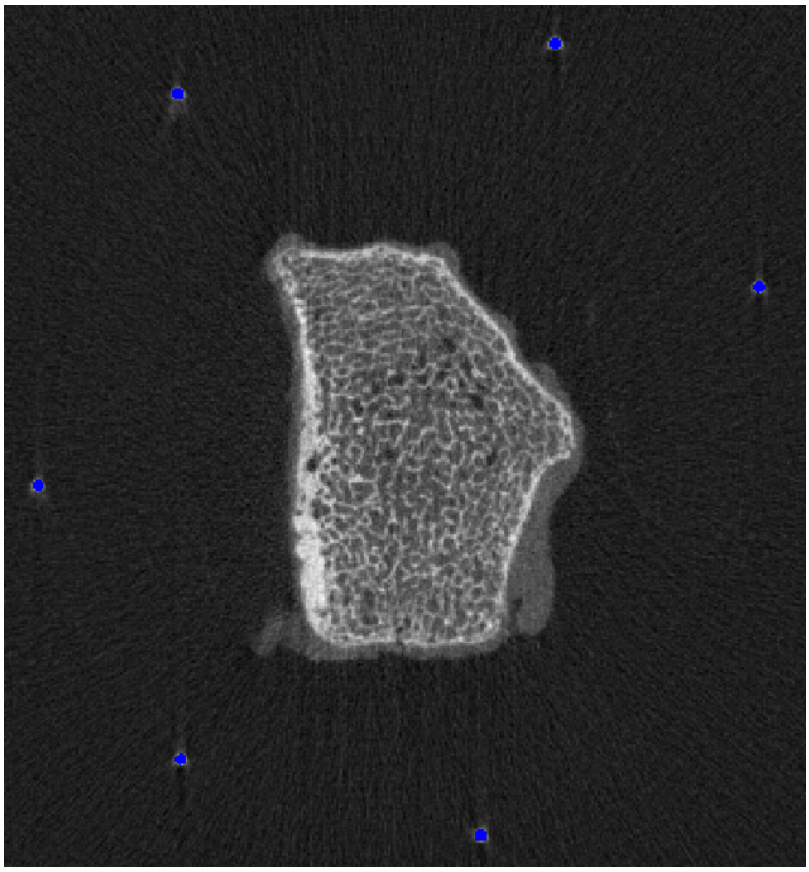

Figure 37 : Superimposition of the extracted landmarks and the reconstructed image.

I calculated the root mean square error for this extraction, by doing:

$RMS_{error} = sqrt ((x_1-x_0)^2 + (y_1-y_0)^2)$,

Where A (x_0 , y_0) corresponds to one landmark coordonnate in the reconstructed image,

And B (x_1 , y_1) corresponds to the landmark position in the result image.

The root mean square errors for the actual sinograms was below equal to zero for most landmark, one landmark however had a coordonnate in the result image that was different from a pixel from its coordonnate in the reconstructed image. This result is acceptable as it will not lead to the generation of an ideal sinewave too different from the actual one.

The main reason source of error in the algorithm is at the step where I need to access the centroid of an object. The coordonnates of the centroid have to be rounded to be displayed, which can lead to some minor error of positions.

b) Comment on the algorithm

The region of interest of the reconstructed image had to be redefined, as the corners were hindering the measure in the sinogram image. I decided to get rid of them by selecting a smaller region of interest.

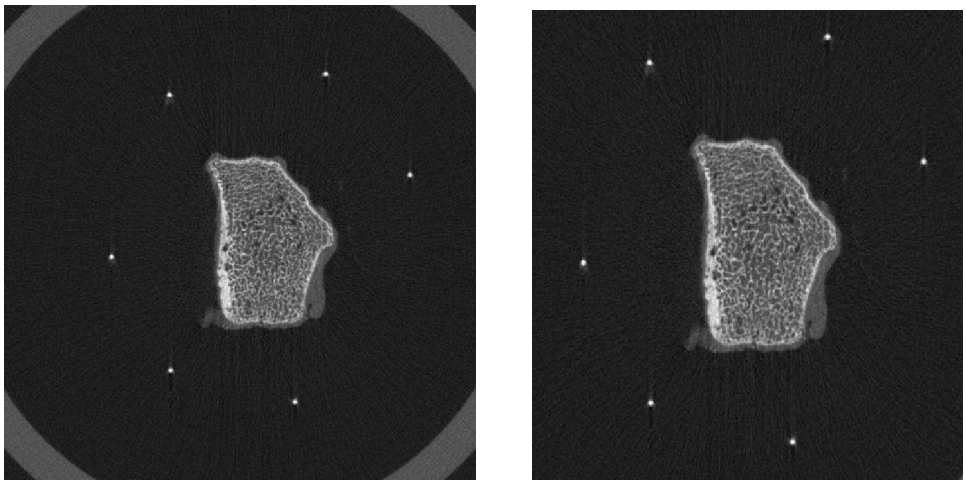

Figure 38 : Selection of the region of interest in the reconstructed image.

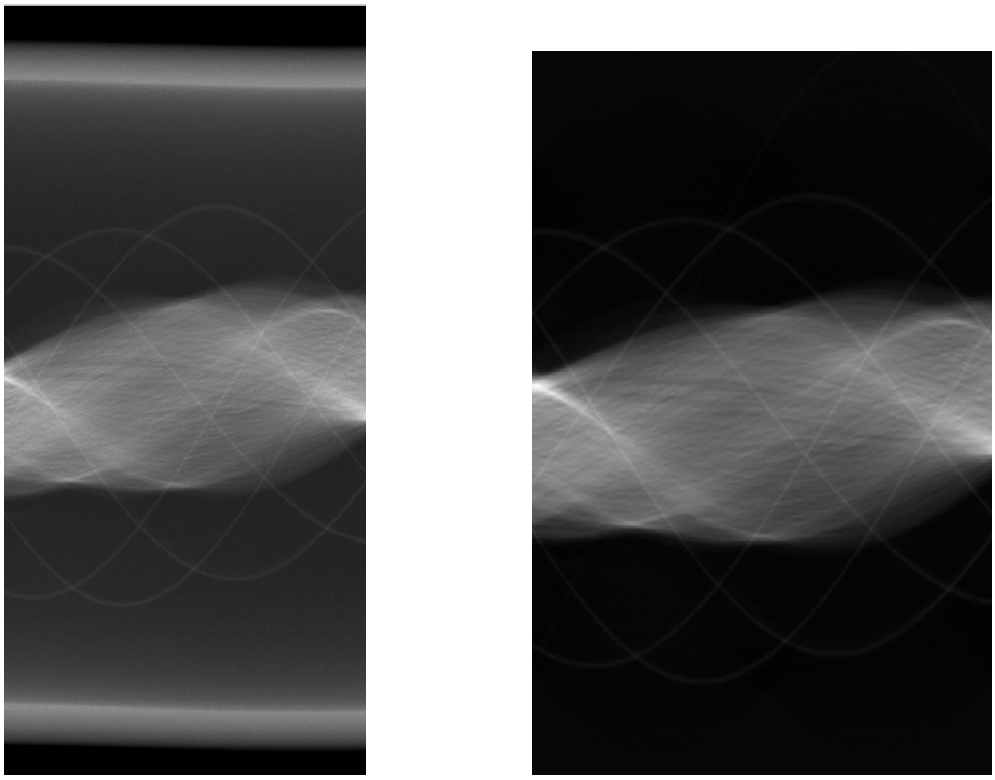

Figure 39 : Consequence for the sonogram of the new region of interest (left: original image, right: sonogram of the new region of interest obtained by inverse Radon transform).

The fact that, I selected a new region of interest by only keeping the landmarks and the cross-section of the wrist, has an impact on the sinogram image. When I perform a Radon transform on the reconstructed image to have the sinogram image I will use in the matching function, the landmark curves in some points are less visible. This, however, does not change the way to process the image.

c) "Funny" fact

In the algorithm, I start working with a sinogram image of size 750*1536 pixels, this image being too big to be displayed; it was resized to half its size (375*768).

The next step in the algorithm is to do an inverse radon transform; the size for the result image (the reconstructed image) is 542*542 pixels.

When going back from the reconstructed image to the sinogram image, e.g. when doing a radon transform on it, it was expected to get an image of the same size as the original sinogram (375*768), but it was not the case. The new sinogram image had a size of 375*771 pixels.

This result was not clearly explained, but we guessed that the origin of the problem was somehow related to the center of gravity for the radon transform in Matlab.

This size problem did not matter then as from the original sinogram image, I do an inverse Radon transform to get the reconstructed image, and from that point I select a zone of interest. So I just need to do one more radon transform on the image to have the sinogram that will be used for the rest of this algorithm, and take the size of this image as the reference.

d) Comment on the parameters used

The aim of the first part of the algorithm was to extract the landmarks position in the reconstructed image.

The main parameters used in this part were the size of the region of interest in the reconstructed image, the size of the median filter, the structuring element for the closing and the size upon which objects would be terminated.

- Region of interest: the region of interest was selected in the reconstructed image. It has a square shape containing the different landmark positions. The size does not matter for the rest of the algorithm as the size of the sinogram we will be working on will be determined by this image.
- Median filtering: the median filtering should not be too big as it tends to put the grey levels to the same level, but there is some flexibility in the choice of this parameter.
- Closing: the structuring element for this step had to be big enough to make the bone architecture merge. A size criteria will be then applied on the objects.
- Size criteria: this parameter defines the objects that will be terminated and those that will not be. The only condition on that parmeter is that it has to be bigger than the surface of a landmark.

The quantity of motion could also be considered as a parameter in the image, as depending on its value, the result of the extraction operations will be changed. A motion too important wil cause the landmarks position to be more spread out than with a smaller motion. This has an effect on the extraction process, as the intensity of the landmark is spread on all the surface of the landmark. The landmark may not be detected as a landmark by the thresholding function.

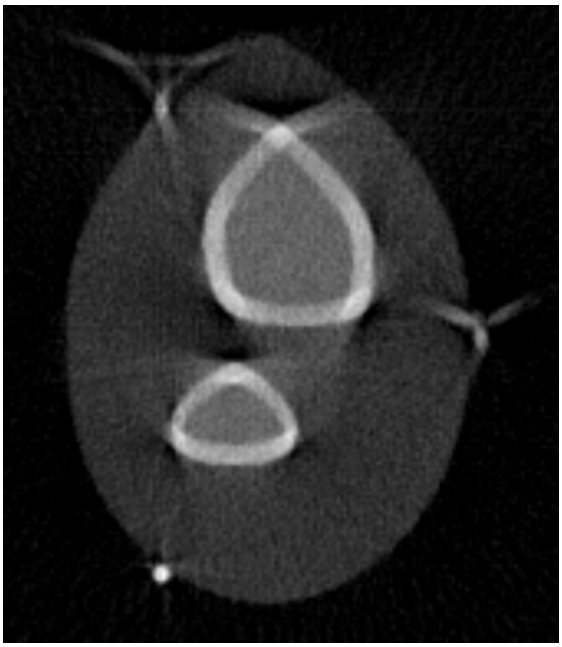

Figure 40 : Effects of severe motion on landmarks in the modelization of a wrist.

e) Results for this step

If these parameters are within working limit, the extraction is feasible and accurate.

The time consumed to extract the landmark position from the reconstructed image is less than a minute in Matlab. This time can be reduced by implementing the algorithm in C++. The most time-consuming steps of the algorithm being the Radon and inverse Radon transform and the opening of the DICOM file.

By taking the Radon transform on the result image, we get the ideal sinewave that is supposed to be the mean value of the landmark curve. If patient motion occurs during the scan, the actual landmark curve position should be found in the immediate neighborhood of the sinewave.

The extraction process has to be accurate as a mistake could lead to a sinewave that would have different properties in term of amplitude and phase shift. The calculation of the root mean square indicates that there should not be any problem. This is confirmed by the visual inspection.

The generated sinewaves matche the landmark curve position in the sinogram.

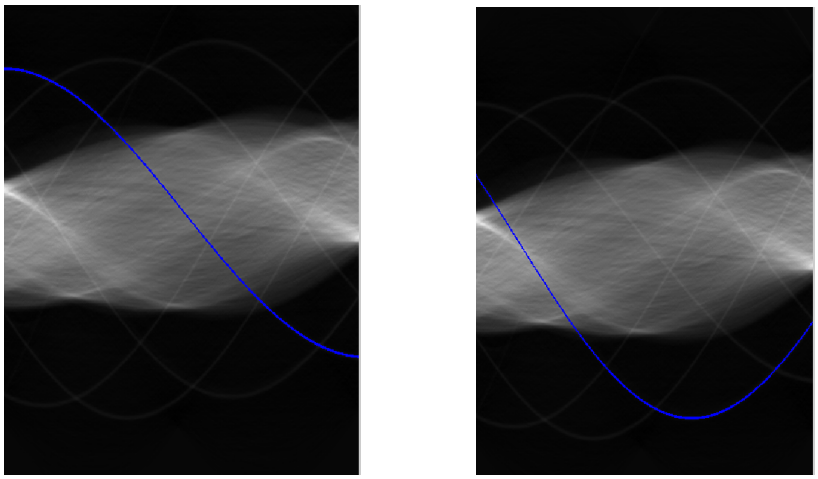

Figure 41 : Generatd sinewave for landmark 1&2.

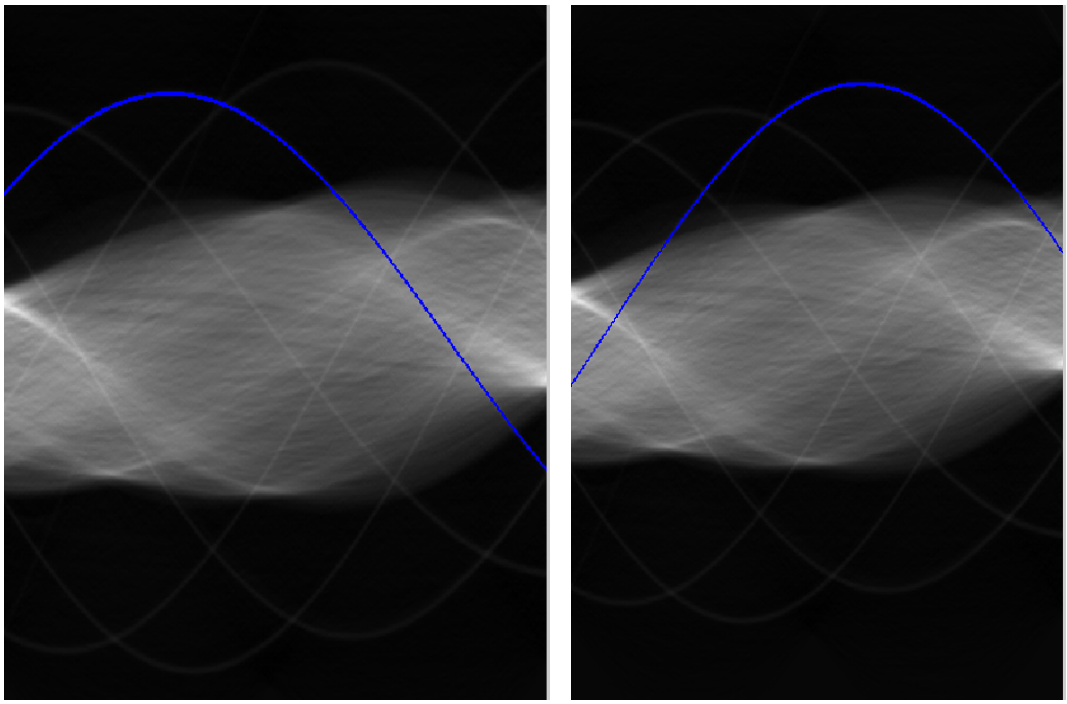

Figure 42: Generated sinewave on landmark 3 & 4.

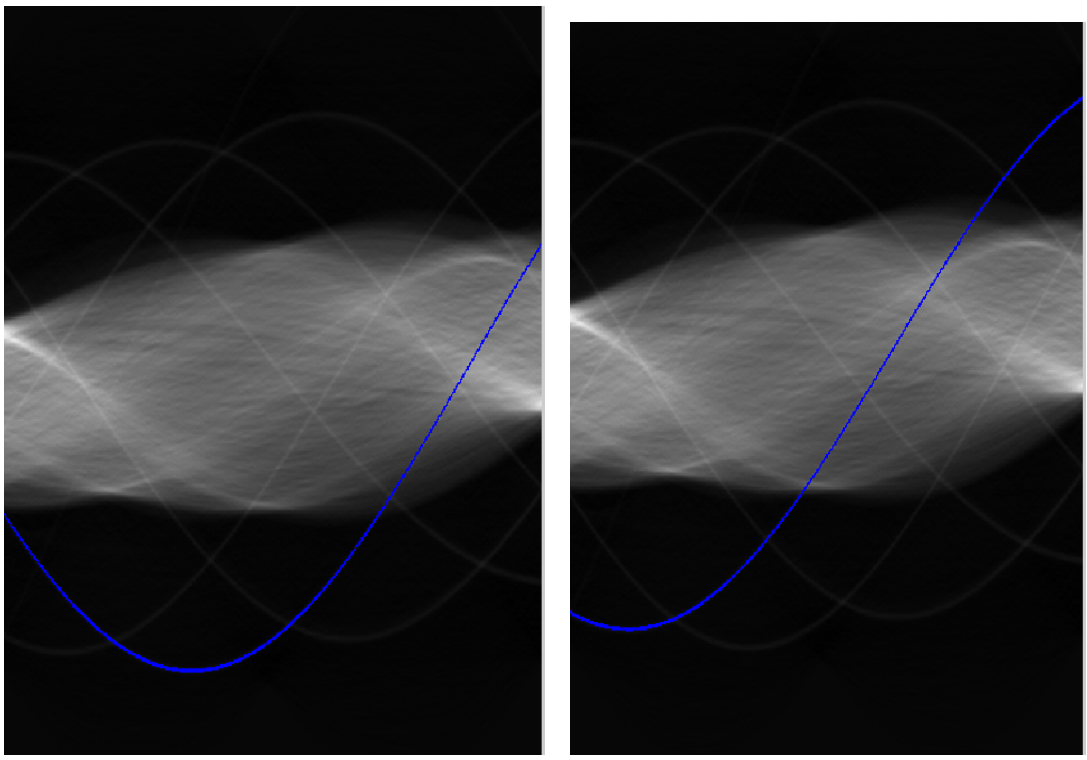

Figure 43 : Generated sinewave on landmark 5 & 6.

7.2. Extraction of the landmark curves

The second step of the algorithm consists in using the ideal sinewave (generated thanks to the first algorithm) as an indication for where to find the actual position of the landmark curve in each projection. The actual position of the landmark curve should be found in the close neighborhood of the sinewave (in the search window), and it should also be a local maximum, as the landmarks are high density. In order to find which local maximum of the search window corresponds to the actual position of the landmark curve position in the projection, a matching function is used. Given that we know the coordonnates of the landmark curve at projection i, the position at projection i+1 can be found using the ideal sinewave, the search window, the hypothesis that it is a local maximum and the fact that from one projection to the next one, the properties of the landmark curve should not change by much.

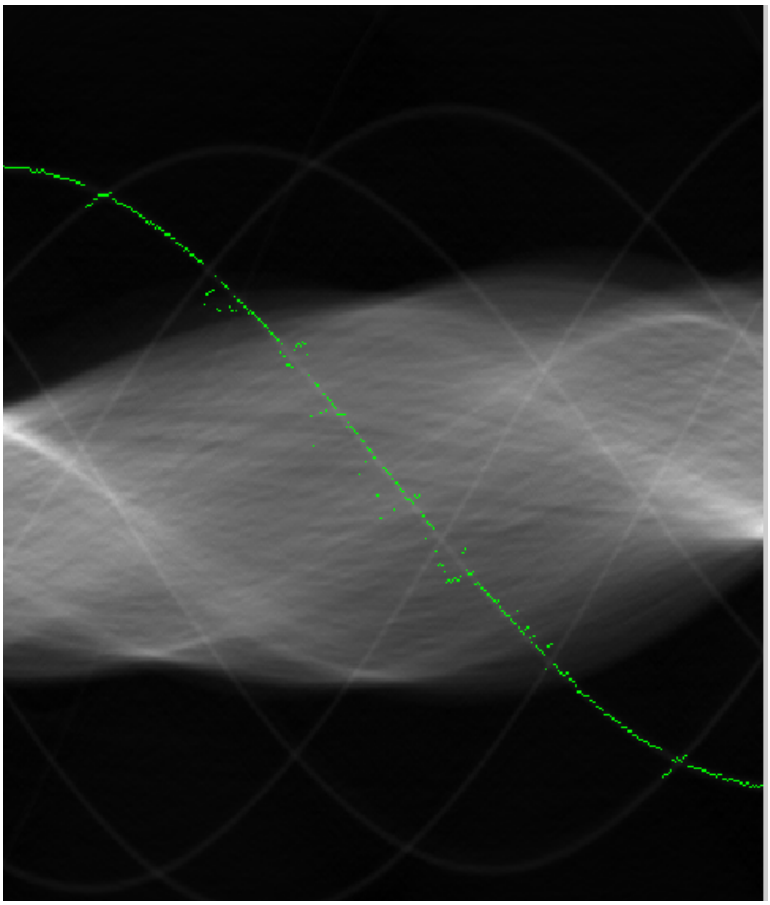

Figure 44: Landmark curve extracted (green), parameters used: search window of 41, tolerance of 70.

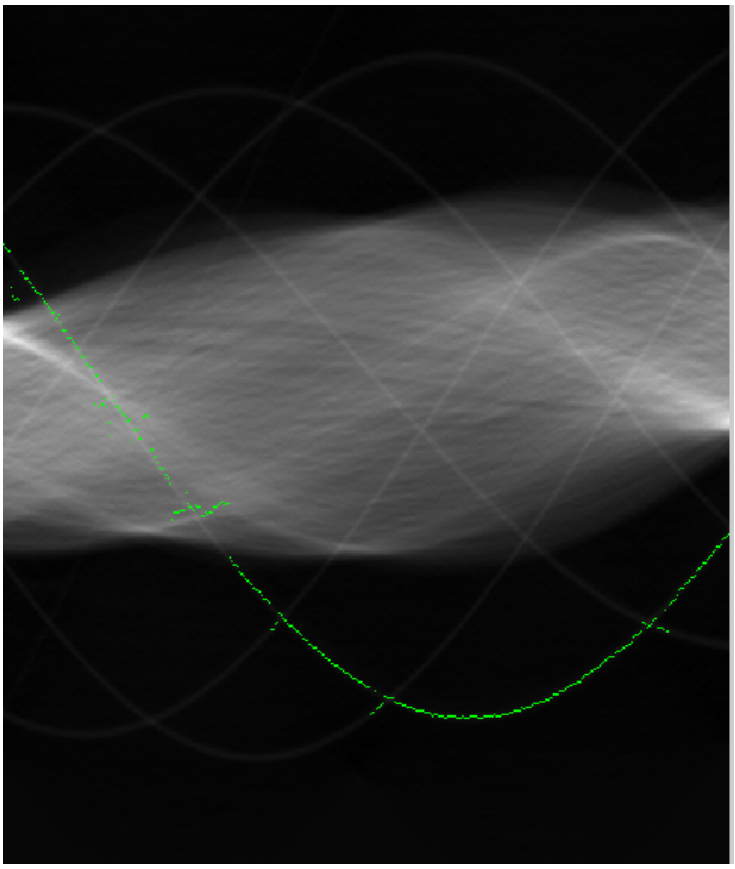

Figure 45 : Landmark Curve extracted in green for a second landmark, same parameters.

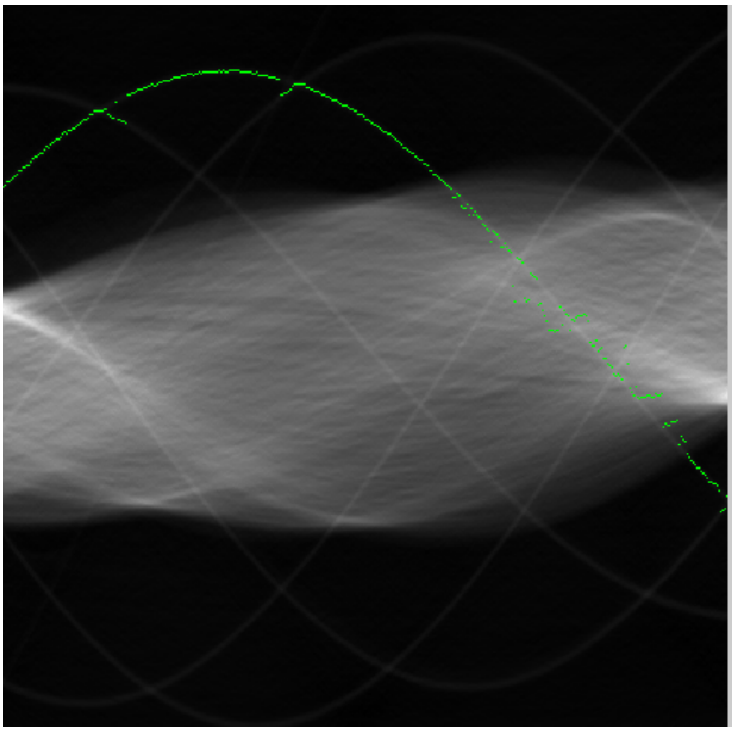

Figure 46 : Landmark Curve extracted in green for a third landmark, same parameters.

a) Size of the search window

The size of the search window is a key parameter in the extraction of the landmark curve.

This element is fundamental as it is a column vector where the actual position for the landmark curve is expected to be found. The actual position of the landmark curve should be a local maximum of this vector.

The bigger the search window will be, the more likely we are to find the actual position of the landmark curve in it.

However, the bigger the search window will be, the more the number of possible locations will be big, which will make the extraction process more time-consuming and also less accurate.

A compromise will have to be found, whether to know if the size of the search window should be augmented to make sure that the actual landmark curve position is present in the column vector or if the quality of the extraction process should be priviledged by limiting as much as possible the number of possible locations in the search window.

After studying several set of images with different motions (axial, continuous, etc), I have been able to quantify the average distance between the ideal sinewave and the actual position for the considered projection.

The average distance between the actual projection and the position the landmark curve would have without motion is 6 pixels in average. As we want to make sure that the landmark curve position is within the search window, I decided to use a search window with a size of 20 pixels from each sides of the sinewave, so 41 pixels in total (2*20 + 1).

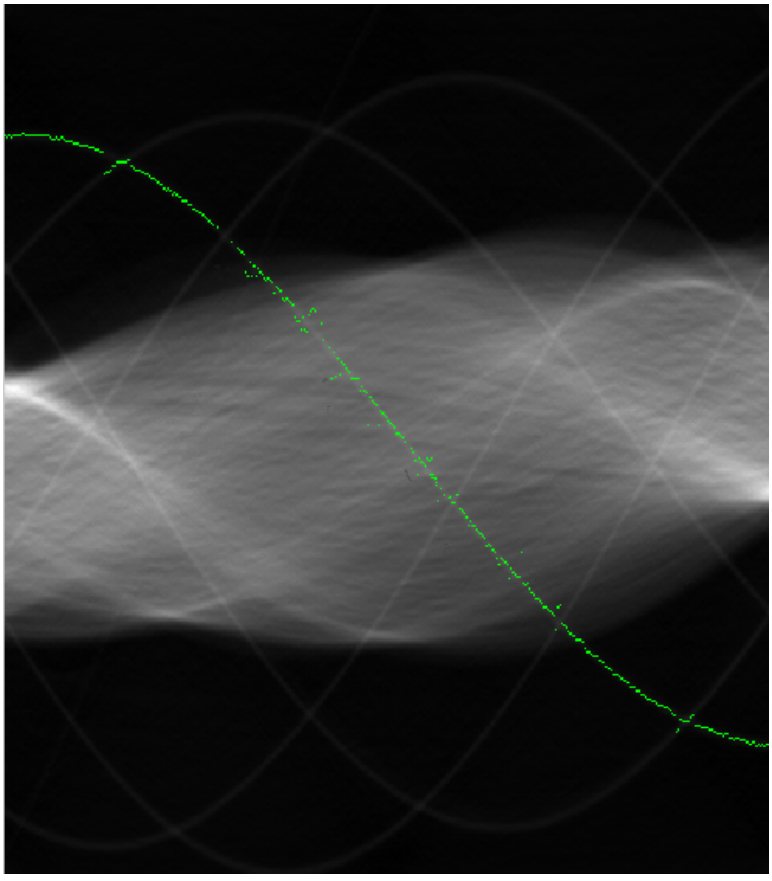

Figure 47 : Extracted landmark curve with different parmeters (size of the search window : 10, tolerance 70).

b) Tolerance of the matching function

The matching function is another important part of the extraction algorithm. The bigger the tolerance will be, the more likely the algorithm will work without using the default criterion, but the consequence is that the matching function can be mistaken. On the contrary, a smaller tolerance for the matching function will lead to the intensive use of the default criterion, as the function was not able to match the result with the previous pixel intensity.

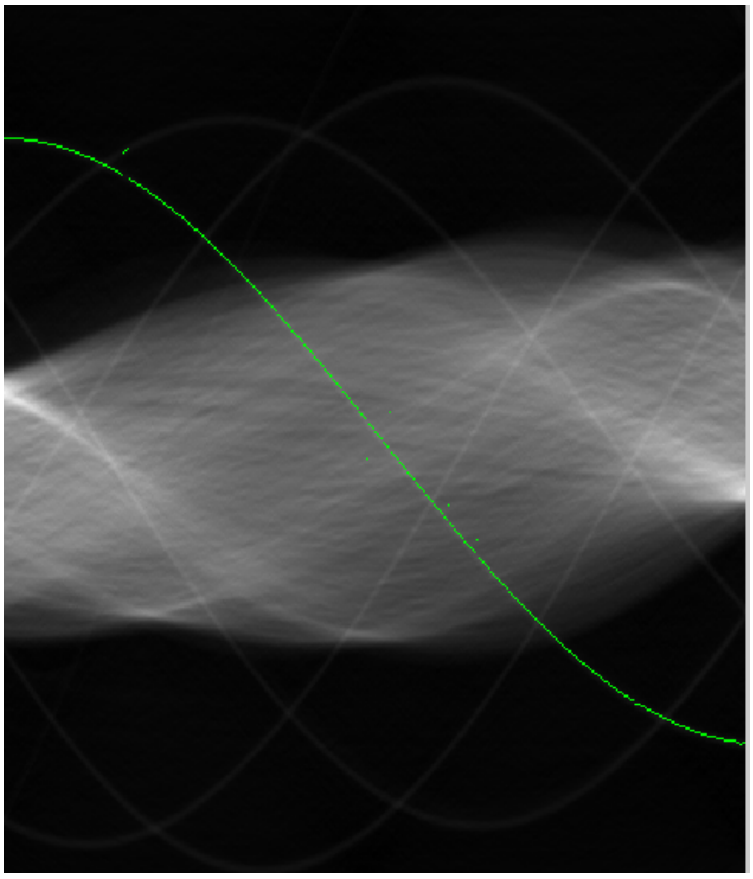

Figure 48: Extracted landmark curve with different parameters (search window of 41, tolerance of 20).

c) Results for this step

The result of the final extraction of the landmark curve is highly depending on the choice of the parameters for the size of the search window and the tolerance of the matching function.

From the input image, to the output result (the landmark curves extracted by the algorithm), the algorithm required about a minute to work.

The extraction was done almost automatically; the only time the user intervened was when I needed to select the new region of interest in the reconstructed image, which actually could have been done automatically.

The output result for the extracted landmark curve can be displayed on the original sinogram image to be submitted for visual inspection, or it can be displayed in a vector, to access the position of the landmark curve for each projection.

I added a function that tells for the desired projection, if the matching function was used or the default criteria. This function is called degree of confindence and returns a "1" when the matching function worked properly and a "0" else.

The ratio for the degree of confidence over the number of projections for the landmark curves extracted, with a total size for the search window of 41 and a tolerance for the matching function of 70 is, depending on the landmark curve, between 1/3 and 1/5. which means that every 3-5 times the algorithm extract a position for the landmark curve, in one case, the landmark curve position was extracted using the default criteria.

Important note: The fact that the default criterion was used does not mean that the extraction is innacurrate.The default criteria can be used and yet produce a good extraction. In the same way, the fact that the matching function was used does not mean that the extraction was accurate (the matching function can be mistaken some times by a pixel with a similar intensity but that does not correspond to a landmark curve position).

Conclusion

The objective of the project was to extract landmark curves in a sinogram as automatically as possible.

Because of the complexity of the image, I decided to work on an algorithm that would extract the landmark curves position on the reconstructed image, generates a sinewave from this extracted points (the sinewave is the mean value of the landmark curve position) and uses an other algorithm to eventually detect the actual landmark curve position. Once a landmark curve position is extracted, the second algorithm will create in the following projection a window search, centered on the position of the ideal sinewave, where the actual position of the landmark curve should be a local maximum. The selection of the actual position is actually completed by doing a match between the intensity of the previously extracted landmark and the local maximums of the search window.

The results obtained are interesting as the extraction operation is done automatically (as desired) and the extracted landmark curve position most of the times correspond to the actual landmark curve position. However, the landmark curve position extracted does not always fit the actual position and a default criterion has to be used in some cases to carry out the extraction process, putting incertainty on the position extracted.

These errors in the extraction process or in the final result are mainly due to the lack of characterizing of the landmark curves properties and therefore by the hyposthesis of work that were made (hypothesis of the search window, hypothesis of the local maximums, and the relative continuity of the landmark curve positions in intensity).

I think that the part leading to the extracton of the landmarks position and the generation of the sinewave should be kept, as it gives some precious information on where to expect the motion in the sinogram image.

However, the second algorithm using the hypothesis of work that leads to the extraction of the landmark curve in the sinogram, should be modified in some way, either by adding criterias to determine which pixel of the search window is the most likely to be the actual landmark curve or by changing the algorithm.

It seems clear from the preceding experiments that a successful approach for landmark detection must consider the presence of the landmark in all projections simultaneously, rather than trying to locate the landmark isolatedly in each projection. Future developments must consider a model for the appearance of the landmark in the sinogram as a whole, in the presence of well-defined classes of motion. In such framework, the motion is obtained from the sinogram as an inverse problem, through the fitting of parameters that lead to the optimal fitting of the landmark model into the actual sinogram.

8. Bibliography

[1] KAK Avinash and SLANEY Malcolm, *Principles of Computerized Tomographic Imaging*, Philadelphia, SIAM, July 2001.

[2] Yu H, Wei Y., Hsieh J, Wang G. (2006) "Data Consistency Based Translational Motion Artifact Reduction in Fan-Beam CT" IEEE Transactions on Medical Imaging, Vol.25, No. 6.

[3] SEERAM Euclid, *Computed Tomography: physical principles, clinical applications and quality control, second edition*, Philadelphia, SAUNDERS, 2001.

[4] BOYD Steven and Pauchard Yves, *Landmark based compensation of patient motion artifacts in computed tomography,* Calgary.

[5] BARRET JF and KEAT N, *Artifacts in CT : Recognition et Avoidance*, RadioGraphics, 2004

[6] Ritchie, C.J. Crawford, C.R. Godwin, J.D. King, K.F. Yongmin Kim (1996) "Correction of computed tomography motion artifacts using pixel-specific back-projection" IEEE Transactions on Medical Imaging Volume: 15, Issue: 3 On page(s): 333-342.

[7] Pauchard Y. and Boyd S.K. (2007) "Landmark based compensation of patient motion artifacts in computed tomography" in SPIE International Symposium, Medical Imaging, submitted

[8] Weiguo Lu and Mackie, T.R. (2002) "Tomographic motion detection and correction directly in sinogram space" Physics in Medicine and Biology, v 47, n 8, p 1267-84

[9] Zerfowski, D (1998) "Motion artifact compensation in CT" Proceedings of the SPIE - The International Society for Optical Engineering, v 3338, pt.1-2, p 416-24

[10] Chao-kung Yaug;Stelios C. Orphaou Sakis; John W Strohbehn "A simulation study of motion artifacts in computed tomography" Physics in Medicine and Biology, 1982,Vol 27,No .1 , 51-61

[11] Ritchie C.J, Peterson E., Yee D.,Kim Y. Ph.D, Gpdwin J.D. M.D., Crawford C.R. Ph.D. (1989) "A 3-d motion control system for the simulation of CT motion artifacts" Proceedings of the Annual International Conference of the IEEE Engineering 9-12 Nov 1989 Page(s):487 - 488 vol.2

[12] ImPACT, Page last checked on March 13, 2008, http://www.impactscan.org/slides/impactcourse/artefacts/img1.html.

[13] WIKIPEDIA, Page last checked on March 13, 2008, http://en.wikipedia.org/wiki/Computed_tomography.

[14] KAZANTSEV I.G, *Tomographic artefacts suppression via backprojection operator optimization,* Page last checked on March 13, 2008, http://ieeexplore.ieee.org/iel3/4140/12183/00559607.pdf?tp=&arnumber=559607&isnumber=12183.

Mots clefs

Artéfacts de movement, tomodensitographie, sinogramme, image reconstruite

Résumé

Les avançées technologiques en tomodensitographie permettent une restitution sans précédente de l'architecture osseuse en 3D des os humains. En raison de la forte résolution des données, tout mouvement pendant le scanner déteriore la qualité de l'image. Le laboratoire d'imagerie osseuse de l'université de Calgary travaille actuellement à quantifier et compenser les mouvements des patients en plaçant des marqueurs sur la peau des patients avant le scanner et suivre les courbes de ces marqueurs de position dans les données des projections de scanner (sinogramme). Le projet consiste à implémenter divers algorithmes permettant l'extraction de manière automatique des courbes de marqueurs dans les sinogrammes en deux ou trois dimensions. Cela fournira une information qualitative sur le fait de savoir si les scanners des patients sont suffisament sans artéfacts de mouvements et peut être permettra de corriger les mouvements survenus durant la procédure de scanner.

Keywords

Motion artifacts, computed tomography, sinogram, reconstructed image

Summary

The recent introduction of high resolution peripheral quantitative computed tomography, allows unprecedented insight into 3D human bone architecture. Due to the high resolution nature of this data, any patient motion during scanning has a detrimental affect on image quality. We are in the process of developing a patient motion detection system, and we have determined that patient motion can be quantified and compensated by placing artificial landmarks on the patients skin prior scanning and tracking the position of each landmark in the acquired CT projection data (sinogram). The project consists of implementing appropriate image processing algorithms to extract the landmark position in the sinograms. The ultimate goal is to provide (semi) automatic landmark position extraction in 2D and 3D sinograms. This will provide a quantitative basis to decide whether patient scans are sufficiently free of motion artifacts, and possibly a basis to correct motions that have occurred during the scanning procedure.

Institut supérieur d'ingénieurs de Saint-Etienne